Published for SISSA by Springer

Received: *July 26, 2016*
Accepted: *October 27, 2016*
Published: *November 10, 2016*

The last gasp of dark matter effective theory

Sebastian Bruggisser,[a] **Francesco Riva**[b] **and Alfredo Urbano**[b]

[a] *DESY,*
Notkestrasse 85, D-22607 Hamburg, Germany
[b] *CERN, Theoretical Physics Department,*
Geneva, Switzerland

E-mail: sebastian.bruggisser@desy.de, francesco.riva@cern.ch, alfredo.leonardo.urbano@cern.ch

Abstract: We discuss an interesting class of models, based on strongly coupled Dark Matter (DM), where sizable effects can be expected in LHC missing energy (MET) searches, compatibly with a large separation of scales. In this case, an effective field theory (EFT) is appropriate (and sometimes necessary) to describe the most relevant interactions at the LHC. The selection rules implied by the structure of the new strong dynamics shape the EFT in an unusual way, revealing the importance of higher-derivative interactions previously ignored. We compare indications from relic density and direct detection experiments with consistent LHC constraints, and asses the relative importance of the latter. Our analysis provides an interesting and well-motivated scenario to model MET at the LHC in terms of a handful of parameters.

Keywords: Effective field theories, Cosmology of Theories beyond the SM, Global Symmetries, Spontaneous Symmetry Breaking

ArXiv ePrint: 1607.02475

doi:10.1007/JHEP11(2016)069

JHEP11(2016)069

Contents

JHEP11(2016)069

1 Motivation

Most of the information we have on Dark Matter (DM) is about exclusions and constraints. In fact, beside evidence for its existence through the gravitational force, DM has not been observed through any other interaction. Yet, these constraints have refined our perspective on the dark sector, excluding baryonic DM, neutrinos and putting severe constraints on the prototype electroweak WIMP. Collider experiments add to the list. In principle, they constitute an important part of the DM search program, because uncertain astrophysical parameters play here a negligible rôle. Unfortunately, however, the information from collider constraints is at times analyzed in a way that hinders a transparent physical interpretation, so that a clear picture of what we have learned from colliders, is still missing. On the one hand an effective field theory (EFT) analysis provides an interesting tool to present these constraints in a rather model-independent fashion, in terms of a handful of relevant parameters [1–5]. On the other hand, it is well known that the large kinematic range accessible at the LHC complicates a consistent EFT analysis, so that specific or simplified models seem to be necessary. Here we take the point of view that neither choice is ideal, but that they rather offer different languages to test different classes of theories. Indeed, the EFT allows, within its realm of validity, to test different broad UV hypotheses. Whenever these hypotheses cannot be tested consistently, simplified models [6–10] can be

more useful.[1] The goal of this article is to sharpen our perspective on where this line has to be drawn. So, instead of exposing situations in which the EFT description is inappropriate (see already ref. [3, 4] or the more recent [13] and references therein for discussions on this issue), we will identify and study the relevant cases where the EFT is useful and necessary.

Simple arguments of power-counting, symmetries and selection rules allow to relate broad properties of the Beyond the Standard Model (BSM) DM sector to specific characteristics of the EFT, without committing entirely to specific models, yet capturing the most relevant features [14–19]. This is enough to reveal that strongly coupled theories give sizable signatures, observable in non-resonant processes, well below the threshold of resonant production of new (mediator) states (see e.g. ref. [20]). This is the perfect target for analyses of LHC DM searches based on an EFT parametrization.

Strongly coupled models have certainly received comparatively little attention in this context, a few reasons that come to mind are the difficulty of performing perturbative calculations at strong coupling (see however [21] for a review of lattice techniques in this context), as well as the observations that both the SM and the DM sectors appear to be weakly coupled at low energies (for DM this is made explicit by the WIMP miracle). Finally, strong coupling might seem at odds with the fact that both the SM fields and the DM that is searched at colliders are inherently light, much lighter than the characteristic scale mediating the SM-DM interaction. Interestingly, all these obstacles are naturally overcome in the presence of *approximate symmetries*. A well-known example are the pions of QCD that, although inherently strongly coupled, they are light and allow at low energy for a perturbative weakly-coupled description through the chiral Lagrangian. This is a consequence of (non-linearly realized) approximate chiral symmetry.

In a companion paper [22], we discuss similar situations, characterized by approximate symmetries in the context of DM, and show that a *generic and complete* description of strongly interacting DM might involve effective interactions in the Lagrangian captured either by *operators of dimension* $D = 6$ *or by operators of* $D = 8$. The approximate symmetries being considered correspond in practice to the case where DM is a pseudo-Nambu-Goldstone Boson (PNGB) — if DM is a scalar — or to the case where DM is a composite fermion or a Goldstino — if DM is a Dirac or Majorana fermion respectively.

Two important novelties characterize the discussion in ref. [22]. First of all is the use of power-counting arguments to estimate the size of coefficients in the EFT expansion, in relation with generic microscopic properties (such as couplings and symmetries). This creates a hierarchy between different coefficients that, in some cases, can go as far as overcoming the suppression associated with the EFT energy expansion: $D = 8$ effects can dominate over $D = 6$ ones. In particular, in well motivated scenarios, high-derivative operators that have not been considered previously in the literature, dominate the collider phenomenology, still within the validity of the EFT description (i.e. $D > 8$ operators are irrelevant). This fact, that required a BSM perspective to be appreciated, opens the door to a new avenue for DM collider searches, that we explore in this article.

[1] Notice that the simplified models proposed so far are themselves EFTs [11, 12], so that the distinction is not so sharp: here we use the mass of the lightest mediator as discriminant.

JHEP11(2016)069

In this work, we study in detail different phenomenological aspects of scenarios based on strong coupling and symmetries, and discuss the consequences of these power-counting rules for DM searches. We compare direct detection (DD) experiments, expectations from the relic density (RD), with LHC constraints from searches of mono-jets and missing energy, and discuss the reliability of our estimates. Indeed, we show explicitly how a strong coupling implies that the EFT description can be used consistently in the context of the LHC, thus avoiding the criticism related to LHC and the DM EFT (see also [23]). On the other hand, we will discuss how, despite the EFT being suitable for LHC analyses, different effective theories are relevant at different energy regimes, thus compromising the comparison with RD and DD experiments. Indeed we show how approximate symmetries imply strong coupling at high-energy, while small symmetry breaking (weakly coupled) effects can dominate at small energy, such as those relevant for DD and RD. This high-energy/low-energy dichotomy will provide a new important ramification in the way we are used to combine information from different experiments, as we show in this paper.[2]

In section 2 we review the effective Lagrangian for DM and its symmetry structure; in section 3 we discuss, in turn, constraints from the LHC, the RD, and DD experiments. Appendix A contains an extensive comparison of our notation (based on Weyl spinors) with the traditional one based on Dirac spinors, as well as additional details of our computations; appendix B describes the collider analysis.

2 An EFT for strongly interacting DM

The EFT is typically associated with an expansion in inverse powers of M, the physical mass scale characteristic of a new sector, so that

$$\mathcal{L} = \sum_{i,D} c_i \frac{{}_D\mathcal{O}_i}{M^{D-4}} \tag{2.1}$$

where ${}_D\mathcal{O}_i$ is a field operator, of mass-dimension D, involving light fields only, which in our case correspond to the SM fields and the DM. Here, c_i's are the Wilson coefficients that scale as

$$c_i \sim (\text{coupling})^{n_i-2}, \tag{2.2}$$

where n_i is the number of fields in the operator ${}_D\mathcal{O}_i$. This behavior eq. (2.2) can be established unambiguously from a bottom-up perspective by restoring the appropriate dimensions in powers of $\hbar \neq 1$ in the Lagrangian[3] [14–18, 20]. In practice, we are mostly interested in operators contributing directly to $SM + SM \to DM + DM$, most of which contain 4 fields only: in this case $c_i \sim (\text{coupling})^2$.

[2] In a similar spirit, ref. [24] discusses how Renormalization Group (RG) effects from the high energy scale (relevant for LHC) to the one relevant for DD can flow between different EFTs. The effects we discuss here are however of a different kind and are more prone to model-dependent parameters, thus genuinely compromising the comparison. Moreover, in section 3.3 we argue that RG effects are subdominant w.r.t. symmetry breaking ones.

[3] It is easy to see that $\mathcal{L} \sim \hbar^1$ and fields scale as $\Phi \sim \hbar^{1/2}$, while couplings scale generically as $g_\Phi \sim \hbar^{-1/2}$, so that the genuinely dimensionless expansion parameter is $g_\Phi \Phi$.

JHEP11(2016)069

The expansion in eq. (2.1) is valid only if the condition

$$E/M \ll 1 \tag{2.3}$$

is fulfilled, where E is the relevant energy of the experiment. Now, the problem is that, from a low-energy perspective, we only have access to the combination $\delta \equiv c_i E^{D-4}/M^{D-4}$. So, for an experiment with a given sensitivity to δ, the EFT validity condition eq. (2.3) is fulfilled only for large enough $c_i \gg \delta$ or, in other words (cf. eq. (2.2)) only in theories with a *large enough coupling* [20]. This fact, in combination with the bias that the DM sector be weakly coupled, has led great part of the DM community to distrust analyses based on DM EFT.

In this article we discuss theories with large Wilson coefficients c_i, because the underlying dynamics is strong, so that sizable effects are compatible with the EFT assumption. Discussing strongly coupled theories does not necessarily imply explicit calculations in explicit or simplified models: broad BSM assumptions can be captured by an adequate power counting, such as in eq. (2.2), which allows to estimate the size of EFT Wilson coefficients. This estimate is discussed in a companion paper [22]; here we recall the underlying assumptions:

i) The SM couples to a new sector, characterized by one mass scale $M \gg m_{\rm DM}$, corresponding to the physical masses of resonances in this sector, and one coupling g_* that characterizes the self-coupling of this sector and its coupling to the SM and to DM.[4]

ii) The new sector respects the following (approximate or exact) SM symmetries, namely gauge $\mathrm{SU}(3)_C \times \mathrm{SU}(2)_L \times \mathrm{U}(1)_Y$, CP, Flavour $\mathrm{U}(1)^5$, custodial $\mathrm{SU}(2)_L \times \mathrm{SU}(2)_R$, Baryon $\mathrm{U}(1)_B$ and individual Lepton number $\mathrm{U}(1)_{L_{1,2,3}}$. We will also assume that the new sector respects a DM stabilizing symmetry and that, if DM is a Dirac fermion, it respects DM chiral symmetry.

iii) In addition to these linearly realized symmetries (which are manifest even in the SM), spontaneous symmetry breaking can account for the existence of other symmetries in the broken phase, preserved by the new sector. At high energy such symmetries will be manifest.

The spontaneous breaking of a global symmetry G to a subgroup $H \subset G$ delivers naturally light (P)NGBs, whose leading interactions are characterized by higher derivatives [25, 26]. This is a consequence of nonlinearly realized G/H.

In a similar way, the spontaneous breaking of supersymmetry delivers a light (Majorana) fermion: the Goldstino. In the limit where all other supersymmetric particles are heavy, Goldstino interactions arise first at the level of $D = 8$ operators and involve higher derivatives [27–29].[5]

[4] This simplistic picture with one BSM scale, one BSM coupling, and symmetries, is certainly reductive w.r.t. realistic scenarios, but it represents a good approximation even in systems with multiple scale/couplings, in the limit where one coupling/scale is much larger than the others.

[5] See also ref. [30] and references therein.

JHEP11(2016)069

Fermionic dark matter					
Unsuppressed			**Suppressed**		
Name	Operator	Wilson coeff.	Name	Operator	Wilson coeff.
${}_6\mathcal{F}_\psi^V$	$\chi^\dagger\bar\sigma^\mu\chi\psi^\dagger\bar\sigma_\mu\psi$	$c_\psi^V g_*^2/M^2$			
			${}_6\mathcal{F}_H^S$	$\chi\chi H^\dagger H$	$c_H^S y_t^2 m_\chi/M^2$
			${}_6\mathcal{F}_B^{dip}$	$\chi\sigma^{\mu\nu}\chi B_{\mu\nu}$	$c_B^{dip} g_* m_\chi/M^2$
${}_8\mathcal{F}_\psi^V$	$\chi^\dagger\bar\sigma^\mu\partial^\nu\chi\psi^\dagger\bar\sigma_\mu D_\nu\psi$	$C_\psi g_*^2/M^4$	${}_8\mathcal{F}_\psi^{\not S}$	$\chi\chi\psi\psi H$	$C_\psi^{\not S} g_*^2 y_\psi m_\chi/M^4$
${}_8\mathcal{F}_\psi^{V\,\prime}$	$\chi^\dagger\bar\sigma^\mu\chi D_\nu\psi^\dagger\bar\sigma_\mu D^\nu\psi$	$C'_\psi g_*^2/M^4$	${}_8\mathcal{F}_\psi^{\not S\,\prime}$	$\chi\psi\psi\chi H$	$C_\psi^{\not S\,\prime} g_*^2 y_\psi m_\chi/M^4$
${}_8\mathcal{F}_V$	$\chi^\dagger\bar\sigma^\mu\partial^\nu\chi V^a_{\mu\rho}V_\nu^{a\,\rho}$	$C_V g_*^2/M^4$	${}_8\mathcal{F}_V^{\not S}$	$\chi\chi V^a_{\mu\nu}V^{a\,\mu\nu}$	$C_V^{\not S} g_*^2 m_\chi/M^4$
${}_8\mathcal{F}_H$	$\chi^\dagger\bar\sigma^\mu\partial^\nu\chi D_\mu H^\dagger D_\nu H$	$C_H g_*^2/M^4$			

Table 1. Effective operators characterizing $DM-SM$ interactions at $D=6$ and specific to $2\to 2$ processes for $D=8$, and the largest possible coefficients allowed by our power-counting rules, as discussed in ref. [22]. Operator nomenclature as follows: the subscript denotes what particles DM couples to and the supscript refers to the particular properties of the operator, $\not S$ denotes symmetry breaking effects while S, V, T betray the structure of a scalar, vector or tensor mediator respectively, ^{dip} for dipole-type operators. In the text $c_i(C_i)$ is the Wilson coefficient of the $D=6$ ($D=8$) operator ${}_6\mathcal{F}_i$ (${}_8\mathcal{F}_i$).

These assumptions are respected by the new sector alone, but can be broken by the couplings of the new sector to either the SM or DM. For instance, the SM introduces more than one coupling (violating *i)*) and the hypercharge coupling g' breaks custodial symmetry (violating *ii)*). Similarly, a DM mass breaks chiral symmetry if DM is a Dirac fermion (violating *ii)*) and it breaks the non-linearly realized symmetries if it's a scalar or Majorana fermion (violating *iii)*).

The way this can be put into use is the following. We write the most general effective Lagrangian capturing interactions between the SM and DM (both in the fermion and in the scalar case), including operators up to $D=8$ (the reason for this will become clear a posteriori — see also discussion in [22]). Then, interactions that preserve all the relevant symmetries can be thought as genuinely originating from the strong sector, and the power counting of their coefficients c_i will genuinely follow eq. (2.2), in terms of the strong coupling $c_i \simeq g_*^{n_i-2}$. On the other hand, terms that break one of the symmetries in *ii), iii)* will pay a price proportional to the associated symmetry breaking parameter. For instance, for scalars of mass-squared m^2, terms that break the associated non linearly-realized G/H symmetry will be proportional to m^2/M^2, while for Dirac (Majorana) fermions, terms that break chiral symmetry (non-linearly realized SUSY), will be suppressed by m/M. This is the crucial ingredient for our high-energy/strong-coupling, low-energy/weak-coupling dichotomy: terms that preserve the symmetries have more derivatives and grow at high-energy, while they become small at low-energy, where symmetry breaking effects (which have less energy dependence) can be comparable.

JHEP11(2016)069

Scalar dark matter					
Unsuppressed			**Suppressed**		
Name	Operator	Wilson coeff.	Name	Operator	Wilson coeff.
${}_6\mathcal{S}_\psi^V$	$\phi^\dagger \overleftrightarrow{\partial}_\mu \phi \psi^\dagger \bar{\sigma}^\mu \psi$	$c_\psi^V g_*^2/M^2$	${}_6\mathcal{S}_\psi^{\not s}$	$\lvert\phi\rvert^2 \psi\psi H$	$c_\psi^{\not s} g_*^2 y_\psi/M^2$
${}_6\mathcal{S}_H^S$	$\partial_\mu \phi^\dagger \partial^\mu \phi \lvert H\rvert^2$	$c_H^S g_*^2/M^2$	${}_6\mathcal{S}_H^{\not s}$	$\lvert\phi\rvert^2 \lvert H\rvert^2$	$c_H^{\not s} g_*^2 m_{\phi,H}^2/M^2$
${}_6\mathcal{S}_B^{dip}$	$\partial_\mu \phi^\dagger \partial_\nu \phi B^{\mu\nu}$	$c_B^{dip} g_*/M^2$			
${}_8\mathcal{S}_\psi^T$	$\partial^\mu \phi^\dagger \partial^\nu \phi \psi^\dagger \bar{\sigma}_\mu D_\nu \psi$	$C_\psi^T g_*^2/M^4$			
			${}_8\mathcal{S}_\psi^S$	$\partial^\mu \phi^\dagger \partial_\mu \phi \psi\psi H$	$C_\psi^S g_*^2 y_\psi/M^4$
${}_8\mathcal{S}_V^S$	$\partial^\mu \phi^\dagger \partial_\mu \phi V^a_{\rho\nu} V^{a\,\rho\nu}$	$C_V^S g_*^2/M^4$	${}_8\mathcal{S}_V^{\not s}$	$\lvert\phi\rvert^2 V^a_{\mu\nu} V^{a\,\mu\nu}$	$C_V^{\not s} g_*^2 m_\phi^2/M^4$
${}_8\mathcal{S}_V^T$	$\partial^\mu \phi^\dagger \partial^\nu \phi V^a_{\mu\rho} V_\nu^{a\,\rho}$	$C_V^T g_*^2/M^4$			
${}_8\mathcal{S}_H^S$	$\partial^\mu \phi^\dagger \partial_\mu \phi D^\nu H^\dagger D_\nu H$	$C_H^S g_*^2/M^4$			
${}_8\mathcal{S}_H^T$	$\partial^\mu \phi^\dagger \partial^\nu \phi D_{\{\mu} H^\dagger D_{\nu\}} H$	$C_H^T g_*^2/M^4$			

Table 2. Same as table 1 but for scalar DM, with operators denoted $\mathcal{S}$.

We summarize the results (explained in more detail in ref. [22]), in table 1 when DM is a fermion and in table 2 when it is a scalar, separating suppressed and unsuppressed effects, and using a notation based on Weyl spinors, where the coefficients c_i are matrices mixing different chiralities (appendix A is dedicated to a comparison with Dirac notation). Tables 1 and 2 report the maximal possible value of the Wilson coefficient, where $c, C \simeq O(1)$ but, depending on the particular choice of G/H if DM is a scalar, and depending on whether it is Majorana or Dirac DM if it is a fermion, some terms might be forbidden $c, C = 0$. The most interesting cases are [22]:

- If DM is a Goldstino (see e.g. [31, 32] and the discussion in [22]), $c_\psi^V = 0$, and the only genuinely strong interactions are at $D = 8$ [27–30, 33, 34].
- If DM is a (real) scalar from an abelian SSB pattern $\mathrm{U}(1)/\mathcal{Z}_2$ [35–37], then the $D = 6$ Lagrangian is penalized: $c_\psi^V = c_H^S = c_B^{dip} = 0$ vanish, and $c_\psi^{\not s}$, $c_H^{\not s}$ are further suppressed by m_ϕ^2/M^2.
- For scalar DM, c_ψ^V, c_B^{dip} can be non-vanishing only if (complex) DM originates from a non-abelian SSB, such as $\mathrm{SU}(2)/\mathrm{U}(1)$ [21, 38–41]. On the other hand c_H^S $c_\psi^{\not s}$, $c_H^{\not s}$ are further suppressed, unless the generators associated with DM and those associated with the Higgs do not commute, such as in $\mathrm{SO}(6)/\mathrm{SO}(5)$ [42–44] or larger [45, 46].
- For simplicity, tables 1 and 2 make the optimistic assumptions that SM fermions are fully composite; in case they are only partially composite [47–49], operators involving SM fermions ψ, are suppressed by the degree of compositeness ξ_ψ^2.[6]

[6] In fact in composite Higgs models based on partial compositeness, a favorable situation is when only the right-handed top quark is fully composite [50–52], while the mixing of lighter fermions to the strong sector is suppressed; see ref. [53].

JHEP11(2016)069

- Finally, operators involving gauge-boson field strengths $V_{\mu\nu}$ can be sizable only if the SM gauge boson realize the paradigm of deformed symmetry — *Remedios* — of ref. [19]. If instead the transverse polarizations of gauge bosons are elementary, operators involving two field strengths will be suppressed by $\sim g_V^2/g_*^2$ (and additionally by $\sim g_*^2/16\pi^2$ if the underlying theory is minimally coupled [18]).

A few further remarks are necessary. First of all, for generic Wilson coefficients c_i, tables 1 and 2 include all $D = 6$ (or smaller, depending on notation) operators connecting the SM with a pair of DM fields; partial integration, field redefinitions (that eliminate operators proportional to the leading equation of motion), Bianchi and Fiertz identities, have been used to focus on a smaller set of operators, in agreement with previous literature [54, 55]. The same is true for operators classified as $D = 8$, although in this case we have focussed on direct contributions to $2 \to 2$ scatterings, which typically constitute the most favorable processes to test SM-DM interactions (see ref. [22] for more details on these criteria). If the gauge vectors are composite, however, the additional unsuppressed structures

$$ {}_8\mathcal{L}_{\rm eff}^{\rm DM} = C_\psi^{\rm mono}\frac{g_*^3}{M^4}\chi^\dagger\bar\sigma_\mu\chi\,\psi^\dagger\bar\sigma_\nu T^a\psi V^{a\,\mu\nu} + C_H^{\rm mono}\frac{g_*^3}{M^4}\chi^\dagger\bar\sigma_\mu\chi\,H^\dagger\overset{\leftrightarrow}{D}_\nu\tau^a H\;W^{a\,\mu\nu} \tag{2.4} $$

for fermion DM, and

$$ {}_8\mathcal{L}_{\rm eff}^{\rm DM} = C_\psi^{\rm mono}\frac{g_*^3}{M^4}\phi^\dagger\overset{\leftrightarrow}{\partial}_\mu\phi\,\psi^\dagger\bar\sigma_\nu T^a\psi V^{a\,\mu\nu} + C_H^{\rm mono}\frac{g_*^3}{M^4}\phi^\dagger\overset{\leftrightarrow}{\partial}_\mu\phi\,H^\dagger\overset{\leftrightarrow}{D}_\mu\tau^a HW^{a\,\mu\nu}\,. \tag{2.5} $$

for scalar DM, contribute directly to $SM + SM \to DM + DM + SM$ and could play a rôle in DM searches at the LHC, as we will discuss in the next section.

Secondly, our construction assumes that the SM itself emerges from the new strongly interacting sector, along the lines of refs. [18, 19], a possibility that has only received a partially rigorous phenomenological treatment. Leaving a detailed analysis of this for future work, we envisage here that a small suppression of the SM couplings to the new sector, and an enhancement of the DM ones, might suppress effects in $SM \to SM$ processes in favor of $SM \to DM$ ones (see [56] for a thorough discussion of this in explicit Z' models)

Finally, the reader might wonder why we are not discussing (linearly realized) supersymmetry, as a *raison d'être* for naturally light scalars. The main reason is that our working hypothesis includes in the light spectrum only the SM fields and DM. A spectrum with only a light scalar DM ($m_\phi \sim$ few GeV) and multi-TeV fermionic partners implies however a precise cancellation between the SUSY-preserving and SUSY-breaking mass terms: a tuning analogous in spirit to the μ-B_μ problem in the MSSM with a multi-TeV Higgsino. We believe therefore that this scenario might be a better target for SUSY simplified models, with a complete chiral multiplet in the light spectrum, rather than our EFT description.[7]

3 Comparison with experiments

In this section we discuss the implications of our arguments for DM searches, focussing first on collider experiments (which motivates our analysis in the first place) and turning

[7]Moreover, since SUSY does not commute with custodial symmetry, it is unlikely that the Higgs takes part in strong supersymmetric dynamics in the few TeV range.

JHEP11(2016)069

to DD and the RD below. A global perspective on the results is given in section 3.4, to which the reader can skip if not interested in a schematic discussion of the analysis (details are postponed to appendices A and B). We focus on LHC processes involving light quarks and gluons, which provide at present the best sensitivity in cases where the DM couples to colored particles. Electroweak-DM processes were instead studied in refs. [57–60] in the EFT framework. It will be interesting to extend this to our strongly coupled perspective, that might betray a well-motivated relation between the DM sector and the mechanism of electroweak symmetry breaking. It is plausible that a large DM-Higgs coupling might have more important effects than a weak DM coupling to fermions, and overcome the prejudice that QCD processes have better sensitivity. An additional example is provided by the operators ${}_6\mathcal{S}^S_H$ and ${}_6\mathcal{S}^{\not s}_{\psi,H}$ which, as studied in [43], reveal the importance of symmetry breaking effects for RD and DD computations. We leave a thorough analysis of this to future work.

3.1 Monojet at LHC

At the beginning of section 2 we have highlighted the difficulties of ensuring that DM analyses are consistent with the EFT assumption. These difficulties were of two kind: the conceptual need of relying on BSM assumptions to discuss EFT validity (we have addressed this point above), and the technical need of performing DM searches in a way that keeps track of the information about the relevant energy of the process. We do this using a procedure in which signal samples are repeatedly generated and analyzed with different upper cuts $E = \sqrt{\hat{s}} < M^i_{\rm cut}$ in the center-of-mass energy of the process (see refs. [20, 61] but in particular ref. [23] that discusses this in the context of DM).[8] For each cut $M^i_{\rm cut}$, a signal σ^{ref} is generated for a given operator for reference values of the parameters $M = 1\,\text{TeV}$, $g_* = 1$, etc , and then rescaled accordingly: for instance the signal of operator ${}_6\mathcal{F}^V_\psi$ scales as $\sigma = g_*^4(1\text{TeV}/M)^4\sigma^{ref}$. In this way, for each $M^i_{\rm cut}$, we can put constraints on EFTs which themselves satisfy $M \gtrsim M^i_{\rm cut}$, in a consistent way. Here we chose to saturate $M = M^i_{\rm cut}$ for illustration, although larger values can be used to increase the reliability of our constraints [20]. This allows us to extract for every operator ${}_D\mathcal{O}_i$ consistent constraints in the plane (M, c_i) where c_i is the Wilson coefficient, or similarly in the plane (M, g_*), using the power-counting of $c(g_*)$ described in the previous section. The important aspect is that the constraints obtained with this additional cut are always conservative, independently of the specific UV completion, and also for M well within the kinematic range accessible at LHC. This follows from the fact that the signal cross section in the complete theory $\sigma_{\rm true}$ splits as $\sigma_{\rm true} = \sigma_{\rm true}(E > M_{\rm cut}) + \sigma_{\rm true}(E < M_{\rm cut})$, where $\sigma_{\rm true}(E < M_{\rm cut}) \approx \sigma_{\rm EFT}(E < M_{\rm cut})$ is well approximated by the EFT, while $\sigma_{\rm true}(E > M_{\rm cut})$ always contributes positively to the cross section in a given kinematic region, so that

$$\sigma_{\rm true} > \sigma_{\rm EFT}(E < M_{\rm cut})\,, \tag{3.1}$$

and the EFT is always conservative, see ref. [23].

[8] Ref. [62–64] proposed a similar method to estimate a posteriori whether a given measurement based on the EFT parametrization is reliable. Moreover, as noted already in the literature, there are different energy scales that can be associated with the hard process. Here we chose the largest, which is $\hat{s}$ and leads to the most conservative analysis. Other choices (e.g. t), might give stronger constraints, but always imply specific assumptions about the UV physics (for instance [65]), which are not necessarily met in our generic analysis.

JHEP11(2016)069

We use this technique to recast the results of (multi- and) mono-jet searches in association with missing transverse energy at the LHC [66–72]. In practice, we compare the data of ref. [69] with different signal simulations, analyzed assuming different values of the cutoff $M_{\rm cut}$. Technical details of this recast study (which contains some novelties w.r.t. previous literature, due to the presence of multiple hard jets in the original analysis of ref. [69]), are discussed in appendix B. The results are shown in figures 1–4, and discussed in section 3.4 below.

3.2 Relic density

Here we discuss the information that can be extracted on the new sector, from analyses of the RD, according to the standard freeze-out paradigm. In the early universe, DM particles are kept in thermal equilibrium through their interactions with the SM thermal bath, until the thermal kinetic energy of lighter particles drops below kinematic thresholds and the expansion of the Universe dilutes the number density of heavier particles in such a way that their annihilation processes become less and less frequent. Eventually, heavier particles freeze-out and their number density, no longer altered by interaction processes, remains constant. The physics of the freeze-out is well-known, and can be summarized by

$$\Omega_{\rm DM}h^2 \approx \frac{10^{-26}\,{\rm cm}^3/{\rm s}}{\langle\sigma v_{\rm rel}\rangle}\,, \qquad \Omega_{\rm DM}h^2|_{\rm obs} = 0.1199 \pm 0.0027 (68\%\ \text{C.L. [73]}) \tag{3.2}$$

where $\langle\sigma v_{\rm rel}\rangle$ is the thermally-averaged annihilation cross section times relative velocity $v_{\rm rel}$, $\Omega_{\rm DM} \equiv \rho_{\rm DM}/\rho_c$ is the ratio between the energy density of DM and the critical energy density of the Universe, $h \equiv H_0/(100\,{\rm km/s/Mpc})$ is the reduced value of the present Hubble parameter H_0.

The cross section can be written generically as $\langle\sigma v_{\rm rel}\rangle \sim \alpha_{\rm DM}^2/m_{\rm DM}^2$, where $\alpha_{\rm DM}$ has dimensions of a coupling and is evaluated at the relevant scale for freeze-out, given by the total energy in the center of mass frame,[9]

$$\sqrt{s} = \frac{2m_{\rm DM}}{\sqrt{1 - v_{\rm rel}^2/4}} \approx 2m_{\rm DM}, \tag{3.3}$$

where (at freeze-out) $v_{\rm rel} \simeq 1/3$. Then eq. (3.2) reads $\Omega_{\rm DM}h^2 \approx 0.1 \times (0.01/\alpha_{\rm DM})^2 \times (m_{\rm DM}/100\,{\rm GeV})^2$, an expression that lies at the heart of the so-called *WIMP miracle* paradigm: a typical weak-scale coupling $\alpha_{\rm DM} \approx \alpha_{em}$ together with a DM mass of the order of the electroweak scale correctly reproduces the observed abundance in eq. (3.2). For our discussion it is important that the RD probes low-energy scales — as exemplified in eq. (3.3) — where even the inherently-strong (but irrelevant) higher dimension interactions of the previous section appear to be weak [22]. Indeed, a naïve estimate (to be refined later) for unsuppressed $D = 6$ operators (scaling as $\sim g_*^2/M^2$) implies that $\alpha_{\rm DM}^2 \approx g_*^2 s/M^2$ and

$$\textbf{D=6:} \qquad \Omega_{\rm DM}h^2 \approx 0.1 \times \left(\frac{4\pi}{g_*}\right)^4 \times \left(\frac{5\,{\rm GeV}}{m_{\rm DM}}\right)^2 \times \left(\frac{M}{3\,{\rm TeV}}\right)^4 . \tag{3.4}$$

[9] Note that the validity of the EFT during the freeze-out epoch requires $2m_{\rm DM}/\sqrt{1 - v_{\rm rel}^2/4} < M$, a condition that is always fulfilled according to our construction.

JHEP11(2016)069

This clearly shows that a strongly coupled light DM belonging to a new sector around the TeV scale fits well the observed abundance.

Given that at freeze-out $v_{\rm rel} \simeq 1/3$ is a relatively small number, the estimate in eq. (3.4) can be refined with a simple analysis of the non-relativistic limit of DM-DM scattering, searching for velocity-suppressed effects. An expansion of the amplitude in partial waves implies $\sigma v_{\rm rel} = \sum_L a_L v_{\rm rel}^{2L} = a_{L=0} + a_{L=1} v_{\rm rel}^2 + a_{L=2} v_{\rm rel}^4 + \mathcal{O}(v_{\rm rel}^6)$, where the $L = 0$, $L = 1$ and $L = 2$ terms define respectively s-wave, p-wave and d-wave.[10] After thermal averaging at temperature T one obtains,

$$\langle \sigma v_{\rm rel} \rangle = a_{L=0} + 6\, a_{L=1} \frac{T}{m_{\rm DM}} + 60\, a_{L=2} \frac{T^2}{m_{\rm DM}^2} + \cdots \tag{3.6}$$

Since $T \approx m_{\rm DM}/25$, this implies that processes in p-wave are suppressed to $\sim 25\,\%$ w.r.t. s-wave, while d-wave to $10\,\%$.

Whether or not an operator can mediate s-wave scattering, can be inferred from the C and P properties of the state it sources: $C = (-1)^{L+S}$, S being the total spin, and $P = (-1)^{L+1}$ for fermions, $P = (-1)^L$ for bosons (see ref. [74] for a review in the context of DM). In our basis only the following (non-relativistic, in Dirac notation[11]) DM bilinear operators can source a state with the appropriate C and P quantum numbers corresponding to $L = 0$:

$$\text{Fermionic DM:} \quad \bar{\boldsymbol{\chi}}\gamma^i \boldsymbol{\chi}\,, \quad \bar{\boldsymbol{\chi}}\gamma^0\gamma^5 \boldsymbol{\chi}\,, \quad i\bar{\boldsymbol{\chi}}\gamma^5 \boldsymbol{\chi}\,, \qquad \text{Scalar DM:} \quad \partial_\mu \phi^\dagger \partial^\mu \phi\,, \quad \phi^\dagger \phi\,. \tag{3.7}$$

Moreover, it is important to remark that the contributions from operators involving the SM bilinears $\bar{\Psi}\gamma^0\Psi$ vanish for charge conservation, while $\bar{\Psi}\gamma^5\gamma^0\Psi$ vanish in the massless quark limit (since in that case chiral symmetry is exact and the associated current is conserved). Finally, the traceless part of operators involving the tensor structures $\bar{\boldsymbol{\chi}}\gamma^\mu \partial^\nu \boldsymbol{\chi}$ and $\partial^\mu \phi^\dagger \partial^\nu \phi$ has total angular momentum $J = S + L = 2$ and implies that for scalars ($S = 0$) the corresponding amplitudes are d-wave suppressed, while for fermions ($S = 0, 1$) they are at least p-wave suppressed. These remarks are sufficient to keep track of p- and d-wave suppressions in DM annihilation and we summarize their impact in tables 3 and 4.

We can now repeat the estimate of eq. (3.4) for $D = 8$ operators, using $\alpha_{\rm DM} \simeq g_*^2 s^2/M^4$ and taking into account the fact that most of them suffer a p-wave suppression,

$$\mathbf{D = 8:} \qquad \Omega_{\rm DM} h^2 \approx 0.1 \times \left(\frac{4\pi}{g_*}\right)^4 \times \left(\frac{60\,\text{GeV}}{m_{\rm DM}}\right)^6 \times \left(\frac{M}{1\,\text{TeV}}\right)^8 . \tag{3.8}$$

[10] The correspondence between total orbital angular momentum L and velocity $v_{\rm rel}$ can be understood considering the representation of a plane wave propagating with absolute momentum $|\vec{p}|$ in direction θ in terms of Legendre polynomials P_L and spherical Bessel functions j_L,

$$\langle \vec{p}, \theta | \vec{x} \rangle = e^{i|\vec{p}||\vec{x}|\cos\theta} = \sum_{L=0}^{\infty} i^L (2L+1) j_L\left(|\vec{p}||\vec{x}|\right) P_L(\cos\theta)\,. \tag{3.5}$$

The argument of j_L is proportional to the velocity, and for small values $j_L(y) \approx y^L/2^L\Gamma(1+L)$, with $\Gamma(z)$ the Gamma function; hence the expansion in powers of $v_{\rm rel}^{2L}$ in the non-relativistic limit.

[11] When discussing RD and DD, we use Dirac, rather than Weyl notation, in order to comply with the relevant literature on the subject; a detailed translation can be found in appendix A.

JHEP11(2016)069

Fermionic dark matter				
DM-SM interaction		**RD**	**DD**	**LHC**
Effective operator	chiral decomposition	$\sigma v_{\rm rel}$	$\sigma_{\rm SI}$	$\mathcal{A}$
Composite fermions				
$\frac{g_*^2}{M^2}\chi^\dagger\bar\sigma^\mu\chi\psi^\dagger\bar\sigma_\mu\psi$	$(\bar{\boldsymbol{\chi}}\gamma^\mu\boldsymbol{\chi})(\bar\Psi\gamma_\mu\Psi)$	$g_*^4 m_\chi^2/M^4$	$g_*^4\mu_N^2/M^4$	$\frac{g_*^2E^2}{M^2}$
	$(\bar{\boldsymbol{\chi}}\gamma^\mu\boldsymbol{\chi})(\bar\Psi\gamma_\mu\gamma^5\Psi)$		×	
	$(\bar{\boldsymbol{\chi}}\gamma^\mu\gamma^5\boldsymbol{\chi})(\bar\Psi\gamma_\mu\Psi)$	$g_*^4 m_\chi^2 v_{\rm rel}^2/M^4$	×	
	$(\bar{\boldsymbol{\chi}}\gamma^\mu\gamma^5\boldsymbol{\chi})(\bar\Psi\gamma_\mu\gamma^5\Psi)$		×	
Goldstino dark matter				
$\frac{g_*^2}{M^4}\chi^\dagger\bar\sigma^\mu\partial^\nu\chi\psi^\dagger\bar\sigma_\mu D_\nu\psi$	$(\bar{\boldsymbol{\chi}}\gamma^\mu\partial^\nu\boldsymbol{\chi})(\bar\Psi\gamma_\mu\overleftrightarrow{\partial_\nu}\Psi)$	$g_*^4 m_\chi^6 v_{\rm rel}^2/M^8$	$\frac{g_*^4\mu_N^2 m_\chi^2 m_N^2}{M^8}$	$\frac{g_*^2E^4}{M^4}$
	$(\bar{\boldsymbol{\chi}}\gamma^\mu\partial^\nu\boldsymbol{\chi})(\bar\Psi\gamma_\mu\gamma^5\overleftrightarrow{\partial_\nu}\Psi)$		×	
	$(\bar{\boldsymbol{\chi}}\gamma^\mu\gamma^5\partial^\nu\boldsymbol{\chi})(\bar\Psi\gamma_\mu\partial_\nu\Psi + h.c.)$		×	
	$(\bar{\boldsymbol{\chi}}\gamma^\mu\gamma^5\partial^\nu\boldsymbol{\chi})(\bar\Psi\gamma_\mu\gamma^5\partial_\nu\Psi + h.c.)$		×	
$\frac{g_*^2}{M^4}\chi^\dagger\bar\sigma^\mu\chi[(D_\nu\psi^\dagger)\bar\sigma_\mu(D^\nu\psi)]$	$(\bar{\boldsymbol{\chi}}\gamma^\mu\gamma^5\boldsymbol{\chi})[(\partial^\nu\Psi)\gamma_\mu(\partial_\nu\Psi)]$	$g_*^4 m_\chi^6 v_{\rm rel}^2/M^8$	×	
	$(\bar{\boldsymbol{\chi}}\gamma^\mu\gamma^5\boldsymbol{\chi})[(\partial^\nu\Psi)\gamma_\mu\gamma^5(\partial_\nu\Psi)]$		×	
$\frac{g_*^2}{M^4}\chi^\dagger\bar\sigma^\mu\partial^\nu\chi V^a_{\mu\rho}V^{a\,\rho}_\nu$	$\bar{\boldsymbol{\chi}}\gamma^\mu(\partial^\nu\boldsymbol{\chi})V^a_{\mu\rho}V^{a\,\rho}_\nu$	$g_*^4 m_\chi^6 v_{\rm rel}^2/M^8$	$\frac{g_*^4\mu_N^2 m_\chi^2 m_N^2}{M^8}$	
Composite gluons				
$\frac{g_*^2 m_\chi}{M^4}\chi\chi V^a_{\mu\nu}V^{a\,\mu\nu}$	$\bar{\boldsymbol{\chi}}\boldsymbol{\chi}V^a_{\mu\nu}V^{a\,\mu\nu}$	$g_*^4 m_\chi^6 v_{\rm rel}^2/M^8$	$\frac{g_*^4\mu_N^2 m_\chi^2 m_N^2}{M^8}$	$\frac{g_*^2 m_\chi E^3}{M^4}$
$\frac{g_*^2}{M^4}\chi^\dagger\bar\sigma^\mu\partial^\nu\chi V^a_{\mu\rho}V^{a\,\rho}_\nu$	$\bar{\boldsymbol{\chi}}\gamma^\mu\overleftrightarrow{\partial^\nu}\boldsymbol{\chi}V^a_{\mu\rho}V^{a\,\rho}_\nu$	$g_*^4 m_\chi^6 v_{\rm rel}^2/M^8$	$\frac{g_*^4\mu_N^2 m_\chi^2 m_N^2}{M^8}$	$\frac{g_*^2E^4}{M^4}$
	$\bar{\boldsymbol{\chi}}\gamma^\mu\gamma^5\overleftrightarrow{\partial^\nu}\boldsymbol{\chi}V^a_{\mu\rho}V^{a\,\rho}_\nu$	0	×	

Table 3. Summary table in the case of fermionic DM. We list the effective operators relevant for our phenomenological analysis, together with their chiral decomposition (see appendix A for details). For each operator, in the last three columns we highlight the parametric dependence — as a function of DM mass m_χ, coupling g_*, and effective scale M — of the annihilation cross section times relative velocity $\sigma v_{\rm rel}$ (relevant for the computation of RD), spin-independent (unsuppressed) DM-nucleon elastic scattering cross section $\sigma_{\rm SI}$ (relevant for DD), and scattering amplitude for DM production at the LHC.

Interactions mediated uniquely by $D = 8$ operators are, as expected, rather weak during the freeze-out era and tend to overproduce DM unless M is small enough or the DM is heavy enough. This should however be taken with a grain of salt. First of all, as we will discuss later, as long as these symmetries are not exact, symmetry breaking effects play an important rôle in explicit models. Secondly, information from the RD depends on the detailed cosmological history (e.g. late-time entropy releases can dilute DM overdensity) and should be taken as an indication to orient collider searches, rather than a constraint on the model.

In what follows, we provide detailed expressions of all the relevant cross sections.

Fermionic DM

D=6. At the leading order in the $1/M$ expansion we find only the operator ${}_6\mathcal{F}^V_\psi$, capturing DM interactions with light quarks. In the limit $m_\psi = 0$, in agreement with the scaling

JHEP11(2016)069

Scalar dark matter				
DM-SM interaction		**RD**	**DD**	**LHC**
Effective operator	chiral decomposition	$\sigma v_{\rm rel}$	$\sigma_{\rm SI}$	$\mathcal{A}$
Complex scalar from SU(2) → U(1)				
$c_\psi^V \frac{g_*^2}{M^2}\phi^\dagger \overleftrightarrow{\partial}_\mu \phi\, \psi^\dagger \bar\sigma^\mu \psi$	$(\phi^\dagger \overleftrightarrow{\partial}_\mu \phi)\bar\Psi\gamma^\mu\gamma^5\Psi$	$g_*^4 m_\chi^2 v_{\rm rel}^2/M^4$	$\times$	$\frac{g_*^2 E^2}{M^2}$
	$(\phi^\dagger \overleftrightarrow{\partial}_\mu \phi)\bar\Psi\gamma^\mu\Psi$		$g_*^4\mu_N^2/M^4$	
Real scalar from U(1) → $\mathcal{Z}_2$				
$C_\psi^T \frac{g_*^2}{M^4}\partial^\mu\phi^\dagger\partial^\nu\phi\psi^\dagger\bar\sigma_\mu D_\nu\psi$	$\partial^{\{\mu}\phi^\dagger\partial^{\nu\}}\phi(\bar\Psi\gamma_\mu \overleftrightarrow{D}_\nu\Psi)$	$g_*^4 m_\chi^6 v_{\rm rel}^4/M^8$	$\frac{g_*^4\mu_N^2 m_\phi^2 m_N^2}{M^8}$	$\frac{g_*^2 E^4}{M^4}$
	$\partial^{\{\mu}\phi^\dagger\partial^{\nu\}}\phi(\bar\Psi\gamma_\mu\gamma^5 \overleftrightarrow{D}_\nu\Psi)$		$\times$	
$C_V^S \frac{g_*^2}{M^4}\partial^\mu\phi^\dagger\partial_\mu\phi V^a_{\rho\nu}V^{a\,\rho\nu}$	—	$g_*^4 m_\chi^6/M^8$	$\frac{g_*^4\mu_N^2 m_\phi^2 m_N^2}{M^8}$	
$C_V^T \frac{g_*^2}{M^4}\partial^\mu\phi^\dagger\partial^\nu\phi V^a_{\mu\rho}V^{a\,\rho}_\nu$	—	$g_*^4 m_\chi^6 v_{\rm rel}^4/M^8$	$\frac{g_*^4\mu_N^2 m_\phi^2 m_N^2}{M^8}$	

Table 4. Same as in table 3, but in the case of scalar DM.

in eq. (3.4)

$$\sigma v_{\rm rel}|_{[{}_6\mathcal{F}_\psi^V]^{\mathcal{D}}_{AA}} = \sigma v_{\rm rel}|_{[{}_6\mathcal{F}_\psi^V]^{\mathcal{D}}_{AV}} = \frac{{c_\psi^V}^2 g_*^4 m_\chi^2 v_{\rm rel}^2}{2\pi M^4}\,,$$
$$\sigma v_{\rm rel}|_{[{}_6\mathcal{F}_\psi^V]^{\mathcal{D}}_{VV}} = \sigma v_{\rm rel}|_{[{}_6\mathcal{F}_\psi^V]^{\mathcal{D}}_{VA}} = \frac{{c_\psi^V}^2 g_*^4 m_\chi^2 (6+v_{\rm rel}^2)}{2\pi M^4}\,, \tag{3.9}$$

where the different results correspond to different chiral structures (AA, VV, AV, VA) for the coefficients c_ψ^V, see appendix A. In eq. (3.9) we added to the operator name $[{}_6\mathcal{F}_\psi^V]$ two additional indices outside the square bracket. The lower one refers to the chiral structure, the upper one to the nature — Dirac ($\mathcal{D}$) or Majorana ($\mathcal{M}$) — of the DM particle. The cross sections in eq. (3.9) refer to Dirac DM. If DM is a Majorana particle, the vector bilinear $\bar{\boldsymbol{\chi}}\gamma^\mu\boldsymbol{\chi}$ identically vanishes since $\boldsymbol{\chi}^C = \boldsymbol{\chi}$: in this case the annihilation cross sections corresponding to the operators $[{}_6\mathcal{F}_\psi^V]_{VV}$ and $[{}_6\mathcal{F}_\psi^V]_{VA}$ vanish while that for $[{}_6\mathcal{F}_\psi^V]_{AV}$ and $[{}_6\mathcal{F}_\psi^V]_{AA}$ must be multiplied by a factor of 4 since the number of diagrams in the scattering amplitude — fermions being equivalent to anti-fermions — doubles.

D=8. We consider the $D = 8$ operators in table 1 mediating DM interactions with quarks and gluons. For DM interactions with gluons, $V = G$, the relevant operators are ${}_8\mathcal{F}_G^{\not s}$, which breaks chiral symmetry and is suppressed by the DM mass, and ${}_8\mathcal{F}_G$, which comes in two different chiral structures (V and A — we refer, again, to appendix A for expressions that include the explicit chiral structure). Note that in our analysis we do not include operator involving dual field strengths; as a consequence, CP invariance restricts the spinor contraction $\chi\chi$ in ${}_8\mathcal{F}_G^{\not s}$ to the chiral combination $[{}_8\mathcal{F}_G^{\not s}]_V$ without γ^5. Furthermore, in ${}_8\mathcal{F}_G$ we consider the traceless combination $G^a_{\mu\rho}G^{a\,\rho}_\nu \to G^a_{\mu\rho}G^{a\,\rho}_\nu - \frac{g_{\mu\nu}}{4}G^a_{\rho\sigma}G^{a\,\rho\sigma}$ in order to single out a genuine tensor structure in the gluon field. We find

$$\sigma v_{\rm rel}|_{[{}_8\mathcal{F}_G^{\not s}]^{\mathcal{D}}_V} = \frac{16 {C_V^{\not s}}^2 g_*^4 m_\chi^6 v_{\rm rel}^2}{\pi M^8}\,, \qquad \sigma v_{\rm rel}|_{[{}_8\mathcal{F}_G]^{\mathcal{D}}_V} = \frac{14 C_V^2 g_*^4 m_\chi^6 v_{\rm rel}^2}{3\pi M^8}\,, \tag{3.10}$$

JHEP11(2016)069

while the axial combination

$$\sigma v_{\rm rel}|_{[{}_8\mathcal{F}_G]^{\mathcal{D}}_A} = \frac{2C_V^2 g_*^4 m_\chi^6 v_{\rm rel}^4}{5\pi M^8}\,, \tag{3.11}$$

is d-wave suppressed as can be understood from our arguments below eq. (3.7) (see for more details the discussion before eq. (A.32) in the appendix). As mentioned above, for Majorana fermions the cross sections are four times larger. Notice that the structure $\chi\chi V^a_{\mu\nu}V^{a\,\mu\nu}$ exhibits the same functional dependence on DM mass and coupling if compared with the genuine $D=8$ operator $[{}_8\mathcal{F}_G]_V$. This is due to the fact that the former has an explicit mass suppression due to the chiral breaking in the DM sector, while the derivative couplings in the latter pick up, when contracted with the corresponding external momenta, the DM mass.

For DM interactions with fermions, we focus on the operators ${}_8\mathcal{F}^V_\psi$ and ${}_8\mathcal{F}^{V\,\prime}_\psi$, and neglect operators suppressed by the small SM Yukawas (we have checked that for the case of operators proportional to the top or bottom quark Yukawa, the LHC is not able to provide constraints consistent with the EFT expansion, even in the limit $g_* \sim 4\pi$, for this reason we will not discuss these operators in what follows). Moreover since the most interesting scenario to consider these operators is that in which the DM is a Goldstino, which is a Majorana fermion, it is worth in this case focussing on Majorana DM. Then

$$\sigma v_{\rm rel}|_{[{}_8\mathcal{F}^V_\psi]^{\mathcal{M}}_{VV}} = \sigma v_{\rm rel}|_{[{}_8\mathcal{F}^V_\psi]^{\mathcal{M}}_{VA}} = 2\,\sigma v_{\rm rel}|_{[{}_8\mathcal{F}^V_\psi]^{\mathcal{M}}_{VV}} = 2\,\sigma v_{\rm rel}|_{[{}_8\mathcal{F}^V_\psi]^{\mathcal{M}}_{VA}} = \frac{8C_\psi^2 g_*^4 m_\chi^6 v_{\rm rel}^2}{\pi M^8}\,. \tag{3.12}$$

and

$$\sigma v_{\rm rel}|_{[{}_8\mathcal{F}^{V\prime}_\psi]^{\mathcal{M}}_{AV}} = \sigma v_{\rm rel}|_{[{}_8\mathcal{F}^{V\prime}_\psi]^{\mathcal{M}}_{AA}} = \frac{32C_\psi'^2 g_*^4 m_\chi^6 v_{\rm rel}^2}{\pi M^8}\,. \tag{3.13}$$

Scalar DM

D=6. At the lowest order, interactions with SM quarks arise from the effective operator ${}_6\mathcal{S}^V_\psi$ in table 2, which appears in two versions, depending on the SM fermion chiral structure (eq. (A.3) in appendix A). We neglect the Yukawa-suppressed effect ${}_6\mathcal{S}^{\not s}_\psi$ which (as we commented for the fermion case) cannot be accessed at the LHC; the important impact of this operator for the RD and DD experiments has been discussed in [43] in the context of the SO(6)/SO(5) model.

From our arguments around eq. (3.7), the effects of ${}_6\mathcal{S}^V_\psi$ are always p-wave suppressed for DM-annihilation in the early Universe. Explicitly, in the limit of vanishing fermion masses,

$$\sigma v_{\rm rel}|_{[{}_6\mathcal{S}^V_\psi]^{\mathcal{C}}_A} = \sigma v_{\rm rel}|_{[{}_6\mathcal{S}^V_\psi]^{\mathcal{C}}_V} = \frac{c_\psi^{V\,2} g_*^4 m_\phi^2 v_{\rm rel}^2}{2\pi M^4}\,. \tag{3.14}$$

Note that the operator ${}_6\mathcal{S}^V_\psi$ is non-vanishing only for complex scalar DM. In eq. (3.14), we added an extra upper index to distinguish between real ($\mathcal{R}$) and complex ($\mathcal{C}$) scalar DM.

Finally, it is worth emphasizing that ${}_6\mathcal{S}^V_\psi$ gives the same cross sections obtained for the operators $[{}_6\mathcal{F}^V_\psi]_{AA,AV}$: in the computation of the RD the only difference between scalar and fermionic case is the number of internal degrees of freedom, which equals to 4 for a Dirac fermion and 2 for a complex scalar.

JHEP11(2016)069

D=8. We consider the $D = 8$ operators in table 2 mediating DM interactions with quarks and gluons. As far as interactions with gluons are concerned, we find again two structures, ${}_8\mathcal{S}_G^S$ and ${}_8\mathcal{S}_G^T$. As before, in ${}_8\mathcal{S}_G^T$ the traceless combination $G^a_{\mu\rho}G^{a\,\rho}_{\nu} \to G^a_{\mu\rho}G^{a\,\rho}_{\nu} - \frac{g_{\mu\nu}}{4}G^a_{\rho\sigma}G^{a\,\rho\sigma}$ is understood. We find

$$\sigma v_{\rm rel}|_{{}_8\mathcal{S}_G^S} = \frac{C_G^{S\,2} g_*^4 m_\phi^6 (4 + 5v_{\rm rel}^2)}{4\pi M^8}\,, \qquad \sigma v_{\rm rel}|_{{}_8\mathcal{S}_G^T} = \frac{2C_G^{T\,2} g_*^4 m_\phi^6 v_{\rm rel}^4}{15\pi M^8}\,. \tag{3.15}$$

If compared with the fermionic case in eq. (3.10), note that the operator ${}_8\mathcal{S}_G^S$, responsible for DM interactions with the scalar gluon current $G^a_{\mu\nu}G^{a\,\mu\nu}$, does not suffer from a p-wave suppression. This is a consequence of CP properties of the initial scalar state. The tensor structure ${}_8\mathcal{S}_G^T$, on the contrary, exhibits the expected d-wave suppression.

Interactions with SM fermions are described by the operator ${}_8\mathcal{S}_\psi^T$. Assuming CP invariance, two combinations are possible — V and A — depending on the chiral structure in the SM current,

$$\sigma v_{\rm rel}|_{[{}_8\mathcal{S}_\psi^T]_V} = \sigma v_{\rm rel}|_{[{}_8\mathcal{S}_\psi^T]_A} = \frac{C_\psi^{T\,2} g_*^4 m_\phi^6 v_{\rm rel}^4}{10\pi M^8}\,. \tag{3.16}$$

The annihilation cross sections are d-wave suppressed, as expected given the tensor nature of the SM current in the final state (see our arguments around eq. (3.7) and appendix A).

3.3 Direct detection

DD of DM can occur through elastic scattering between an incident DM particle and a nucleon N in a nucleus at rest inside the detector. Experiments based on a Xenon target — such as XENON [75] and LUX [76, 77] — use liquefied ultra-pure xenon as a scintillator; interactions inside the xenon create an amount of light, subsequently captured by layers of photomultipliers, proportional to the amount of energy deposited. The nuclear recoil energy $E_{\rm NR} = \frac{\mu_N^2 v^2}{m_N}(1 - \cos\theta)$ for which these experiments have maximum sensitivity is of order $E_{\rm NR} \approx 3 \div 25$ keV, where $v \equiv |\vec{v}| = |\vec{v}_{DM,in} - \vec{v}_{N,in}|$ is the relative incoming velocity between DM and nucleon, $\mu_N \equiv m_{\rm DM} m_N/(m_N + m_{\rm DM})$ the reduced mass and θ the scattering angle. Then, assuming a Maxwellian DM velocity distribution with $v_0 = 220$ km/s, escape velocity $v_{esc} = 544$ km/s, and Earth average velocity 245 km/s, gives a lower bound on the DM mass $m_\chi \gtrsim 8\,\text{GeV}$ that can be detected in these experiments. Given how stringent DD constraints can be, this motivates LHC searches for light DM particles that is the primary focus of this article.

More recently, the CDMSLite [78] and CRESST-II [79] experiments lowered the threshold for DM detection. The CDMSLite experiment uses cryogenic germanium detectors to amplify the phonon signal while the CRESST-II experiment uses cryogenic detectors with crystals of calcium tungstate cooled to mK temperatures. As a result, strong competitive limits were obtained for DM mass in the range $1 - 8\,\text{GeV}$.

The typical velocities $v \sim 10^{-3}$ are well within the realm of non-relativistic mechanics, where the kinematics of DM-nucleon scattering can be described by the following quantities: the DM and nucleon mass, $m_{\rm DM}$, $m_n \approx m_p \equiv m_N = 1\,\text{GeV}$ (and their combination, μ_N); the vectors for velocity $\vec{v}$ and momentum transfer $\vec{q}$, and the (parity even) pseudovectors for nucleon and DM spin $\vec{s}_N$, $\vec{s}_\chi$, when DM is a fermion. As a matter of fact, amplitudes

JHEP11(2016)069

that are proportional to $\vec{v}$ or $\vec{q}$ are suppressed and subleading in DD experiments, and we will neglect them.[12] On the other hand, amplitudes proportional to $\vec{s}_N$ contribute only to spin-dependent detection experiments, whose constraints are significantly weaker than spin-independent ones, and will also be ignored. Finally, the $SM + DM \to SM + DM$ amplitudes we are interested in, are at most linear in the DM spin $\vec{s}_\chi$, but rotational invariant combinations that include $\vec{s}_\chi$ necessary include a product with one of the above-cited vectors, and will hence also be neglected.

We are therefore interested in amplitudes that depend at leading order only on the DM and nucleon masses and on none of the above-mentioned (pseudo) vectors. Now, all relativistic operators include, in the non-relativistic limit, a matrix element where the contribution from the DM bilinear transforms as a scalar (e.g. the time-component of $\bar{\chi}\sigma^\mu\chi$) and can potentially have unsuppressed interactions. It is easy to see, however, that all structures that in Dirac notation contain a γ_5 will be odd under parity. In terms of the above-mentioned quantities this can be associated only with the product of a vector ($\vec{v}$ or $\vec{q}$) and a pseudovector ($\vec{s}_N$ or $\vec{s}_\chi$) and is therefore always suppressed (see refs. [80, 81] and [82] for a review). For this reason DD experiments have their largest impact on structures without γ_5 and we shall limit our discussion to those.[13]

Then it is very easy to estimate the size of the unsuppressed contributions to the spin-independent cross section. For $D = 6$ operators we find generically[14]

$$\textbf{D=6:} \qquad \sigma_{\rm SI} \sim \frac{g_*^4 \mu_N^2}{\pi M^4} \approx 10^{-38}\ {\rm cm}^2 \times \left(\frac{g_*}{4\pi}\right)^4 \times \left(\frac{3\,{\rm TeV}}{M}\right)^4 , \tag{3.17}$$

up to numerical $O(1)$ factors that depend on the particular nucleon constituents the DM couples to. Note that in eq. (3.17) the dependence from the DM mass cancels out in μ_N for $m_{\rm DM} \gg m_N \simeq 1\,{\rm GeV}$, a good approximation already for $m_{\rm DM} \gtrsim 10\,{\rm GeV}$. For DM masses above the threshold $m_{\rm DM} \gtrsim 8\,{\rm GeV}$, and M in the multi-TeV regime, this estimate shows that the presence of a strong coupling is not compatible with the typical ballpark of cross sections tested by DD experiments based on xenon detectors [76], which imply

$$\sigma_{\rm SI}|_{\rm obs} \lesssim 10^{-45}\ {\rm cm}^2 . \tag{3.18}$$

This estimate strengthens the connection between light DM — possibly below the kinematic threshold for DD xenon experiments $m_{\rm DM} \lesssim 8\,{\rm GeV}$ — and strong coupling naturally provided by the framework of approximate symmetries [22]. Indeed, in the mass range

[12] See however appendix A.2 for a discussion about their impact if compared with LHC searches.

[13] As discussed in ref. [24], renormalization group (RG) effects from the scale M down to the scale at which the experimental measurements are performed — that is roughly given by μ_N in DD experiments — mix effective operators among themselves (in fact no symmetry, but only selection rules reflecting the UV particle content, forbid the presence of a vector over an axial structure); for instance, the operator $\bar{\boldsymbol{\chi}}\gamma^\mu\boldsymbol{\chi}\bar{\Psi}\gamma_\mu\gamma^5\Psi$ flows to $\bar{\boldsymbol{\chi}}\gamma^\mu\boldsymbol{\chi}\bar{\Psi}\gamma_\mu\Psi$ thus generating a sizable coupling with the vector quark current in the nucleon. In the strongly coupled models we consider here, we expect multiple resonances at the cut-off M with different properties (similarly to QCD), so that in general all structure can be generated in the UV; for this reason we focus on the leading order contributions and neglect RG effects.

[14] In the text we refer to the computation of the DM-nucleon (rather than DM-nucleus) elastic cross section, since the experimental results in [76, 77] are normalized w.r.t. this quantity.

JHEP11(2016)069

$1 \lesssim m_{\rm DM} \lesssim 8\,{\rm GeV}$ limits from CDMSLite [78] and CRESST-II [79] imply $\sigma_{\rm SI}|_{\rm obs} \lesssim 10^{-38} - 10^{-41}$ cm^2, in better agreement with eq. (3.17).

A similar estimate for $D = 8$ operators, whose contribution to the amplitude is suppressed by an additional $m_{\rm DM} m_N / M^2$, gives

$$\textbf{D=8:} \qquad \sigma_{\rm SI} \sim \frac{g_*^4 \mu_N^2 m_{\rm DM}^2 m_N^2}{\pi M^8} \approx 10^{-44}\,{\rm cm}^2 \times \left(\frac{g_*}{4\pi}\right)^4 \times \left(\frac{m_{\rm DM}}{60\ {\rm GeV}}\right)^2 \times \left(\frac{1\ {\rm TeV}}{M}\right)^8 . \quad (3.19)$$

Similarly to calculations for the RD, DD experiments have access to $D = 8$ operators only for rather small M or large enough DM mass. We summarize these estimates in tables 3 and 4 and in what follows we provide more refined expressions. We parallel the sterile presentation from the previous section on RD, and include more details in appendix A. In particular, for completeness, in appendix A.2 we compare mono-jet LHC searches and RD with spin-dependent and suppressed spin-independent DD cross sections.

Fermionic DM

D=6. For operator ${}_6\mathcal{F}_\psi^V$, only the VV structure — non vanishing in the case of Dirac DM — gives relevant constraints, with

$$\sigma_{\rm SI}|_{[{}_6\mathcal{F}_\psi^V]^{\mathcal{D}}_{VV}} = \frac{9 g_*^4 \mu_N^2}{\pi M^4}\,, \quad (3.20)$$

where we assumed equal coupling with up- and down-type quarks, $c_u^V = c_d^V = 1$. Note that this cross section falls in the ballpark estimated in eq. (3.17).

D=8. Similarly, for ${}_8\mathcal{F}_\psi^V$ we consider only the chiral structure that has unsuppressed effects in DD (without γ_5 in Dirac notation). In order to make contact with previous literature on the subject [83], we rewrite it as[15]

$$C_\psi \frac{g_*^2}{M^4} [\bar{\boldsymbol{\chi}}\gamma^\mu(\partial^\nu \boldsymbol{\chi})] \left(\bar\Psi \gamma_\mu \overleftrightarrow{\partial_\nu} \Psi\right) = C_\psi \frac{g_*^2}{M^4} \left\{ \mathcal{O}^\psi_{\mu\nu} [\bar{\boldsymbol{\chi}}\gamma^\mu(\partial^\nu \boldsymbol{\chi})] - \frac{1}{2} m_\Psi m_\chi \bar{\boldsymbol{\chi}}\boldsymbol{\chi}\bar\Psi\Psi \right\} + O\left(\frac{1}{M^6}\right) \quad (3.21)$$

where

$$\mathcal{O}^\psi_{\mu\nu} \equiv \frac{1}{2}\left[\bar\Psi\gamma_\mu(\partial_\nu\Psi) - (\partial_\nu\Psi)\gamma_\mu\Psi + \bar\Psi\gamma_\nu(\partial_\mu\Psi) - (\partial_\mu\bar\Psi)\gamma_\nu\Psi + i m_\Psi g_{\mu\nu}\bar\Psi\Psi\right], \quad (3.22)$$

defines the so-called quark twist-2 operator whose nuclear matrix element $\langle N|\mathcal{O}^\psi_{\mu\nu}|N\rangle$ is known and can be parametrized in terms of the second moments $\psi_{(2)}$ of the parton distribution functions and the coefficients $f_{T_q}^{(N)} \equiv \frac{\langle N|m_\Psi \bar\Psi\Psi|N\rangle}{m_N}$ describing the light quark contribution to the nucleon mass. We obtain

$$\sigma_{\rm SI}|_{[{}_8\mathcal{F}_\psi^V]^{\mathcal{M}}_{VV}} = \frac{g_*^4 \mu_N^2 m_\chi^2 m_N^2}{4\pi M^8} \left\{ \sum_{\psi=u,d,s} \left[3(\psi_{(2)}(\mu_0) + \bar\psi_{(2)}(\mu_0)) + \left(f_{T_u}^{(N)} + f_{T_d}^{(N)} + f_{T_s}^{(N)}\right)\right] \right\}^2 \quad (3.23)$$

[15] Here we use the equivalence resulting from the equations of motion and add a mass-suppressed operator that is always suppressed at high-energy; at low-energy, however, it has an $O(1)$ effect on the result, captured by the last 3 terms in eq. (3.23).

JHEP11(2016)069

where we assumed $C_u = C_d = C_s = 1$. In our analysis we use the numerical values quoted in [84], evaluated at the scale $\mu_0 = m_Z$.[16] Eq. (3.23) is valid in the case of Majorana DM (in [83] the operator in eq. (3.21) was studied in the context of effective neutralino-quark interactions). This is the relevant case in our analysis, since we consider the operator ${}_8\mathcal{F}_\psi^V$ in the context of Goldstino DM.

The operator ${}_8\mathcal{F}'_\psi$, on the other hand, is expected to play a rôle mostly in the Goldstino case, where lower derivative terms are forbidden. In this situation, however, it is always associated with the γ_5 structure (since for a Majorana fermion, like the Goldstino, $\bar{\boldsymbol{\chi}}\gamma_\mu\boldsymbol{\chi} = 0$) and is therefore subdominant in DD experiments.

For interactions with gluons, the effect of the mass-suppressed operator ${}_8\mathcal{F}_G^{\not s}$ is well known; with our power-counting we find

$$\sigma_{\rm SI}\big|_{[{}_8\mathcal{F}_G^{\not s}]_V^{\mathcal{D}}} = \frac{1}{4}\,\sigma_{\rm SI}\big|_{[{}_8\mathcal{F}_G^{\not s}]_V^{\mathcal{M}}} = \frac{C_G^{\not s\,2} g_*^4 \mu_N^2 m_\chi^2 m_N^2}{\pi M^8}\left[\frac{8\pi}{9\alpha_s} f_{T_G}^{(N)}\right]^2 . \tag{3.25}$$

Let us now consider the operator ${}_8\mathcal{F}_G$, absent in previous literature. There are two different chiral structures in the DM current, but only the one without the γ^5 — marked with a sub-index V in the following — gives a stringent spin independent constraint. As already discussed for the computation of the RD, we take the traceless part of $G^a_{\mu\rho}G^{a\,\rho}_\nu$ in order to couple DM with a genuine tensor current. In the jargon of DD, the resulting combination is known as gluon twist-2 operator $\mathcal{O}^G_{\mu\nu} \equiv G^a_{\mu\rho}G^{a\,\rho}_\nu - \frac{1}{4}g_{\mu\nu}G^a_{\rho\sigma}G^{a,\rho\sigma}$. The nuclear matrix element $\langle N|\mathcal{O}^G_{\mu\nu}|N\rangle$ at zero momentum transfer is known in terms of the second moment of the gluon parton distribution function $g_{(2)}(\mu_0)$ (evaluated at the scale $\mu_0 = m_Z$) [84]. We find (see as usual appendix A for a more detailed computation)

$$\sigma_{\rm SI}\big|_{[{}_8\mathcal{F}_G]_V^{\mathcal{D}}} = \frac{1}{4}\,\sigma_{\rm SI}\big|_{[{}_8\mathcal{F}_G]_V^{\mathcal{M}}} = \frac{C_G^2 g_*^4 \mu_N^2 m_\chi^2 m_N^2}{\pi M^8}\left[\frac{3}{2} g_{(2)}(\mu_0)\right]^2 . \tag{3.26}$$

Scalar DM

D=6. At the lowest order, interactions with SM quarks arise from the effective operator ${}_6\mathcal{S}_\psi^V$ in table 2, which appears in two versions, depending on the SM fermion chiral structure (eq. (A.3) in appendix A). For the vector interaction, we find

$$\sigma_{\rm SI}\big|_{[{}_6\mathcal{S}_\psi^V]_V^{\mathcal{C}}} = \frac{9 g_*^4 \mu_N^2}{\pi M^4} , \tag{3.27}$$

where we assumed equal unit coupling with up- and down-type quarks.

D=8. At $D = 8$, we have interactions with quarks and gluons, the former being captured by the operator ${}_8\mathcal{S}_\psi^T$. The computation of $\sigma_{\rm SI}$ closely follow what already discussed for the

[16] Formally, we have

$$\psi_{(2)}(\mu_0) + \bar\psi_{(2)}(\mu_0) \equiv \int_0^1 dx x[\psi(x,\mu_0) + \bar\psi(x,\mu_0)] , \tag{3.24}$$

where $\psi(x,\mu_0)$ and $\bar\psi(x,\mu_0)$ are the parton distribution functions of quark and antiquark in the nucleon at the scale μ_0.

operator ${}_8\mathcal{F}_\psi^V$ since it exploits the properties of the quark twist-2 operator. We find

$$\sigma_{\rm SI}\big|_{[{}_8\mathcal{S}_\psi^T]_V^{\mathcal{C}}} = \frac{1}{4}\,\sigma_{\rm SI}\big|_{[{}_8\mathcal{S}_\psi^T]_V^{\mathcal{R}}} \tag{3.28}$$
$$= \frac{g_*^4\mu_N^2 m_\phi^2 m_N^2}{\pi M^8}\left\{\sum_{\psi=u,d,s}\left[\frac{3}{4}(\psi_{(2)}(\mu_0)+\bar{\psi}_{(2)}(\mu_0))+\frac{1}{2}\left(f_{T_u}^{(N)}+f_{T_d}^{(N)}+f_{T_s}^{(N)}\right)\right]\right\}^2 .$$

Finally, scalar DM interactions with gluons are described by the operators ${}_8\mathcal{S}_G^S$ and ${}_8\mathcal{S}_G^T$. We find

$$\sigma_{\rm SI}\big|_{[{}_8\mathcal{S}_G^S]^{\mathcal{C}}} = \frac{1}{4}\,\sigma_{\rm SI}\big|_{[{}_8\mathcal{S}_G^S]^{\mathcal{R}}} = \frac{g_*^4\mu_N^2 m_N^2 m_\phi^2}{\pi M^8}\left[\frac{8\pi}{9\alpha_s}f_{T_G}^{(N)}\right]^2 , \tag{3.29}$$

$$\sigma_{\rm SI}\big|_{[{}_8\mathcal{S}_G^T]^{\mathcal{C}}} = \frac{1}{4}\,\sigma_{\rm SI}\big|_{[{}_8\mathcal{S}_G^T]^{\mathcal{R}}} = \frac{g_*^4\mu_N^2 m_N^2 m_\phi^2}{\pi M^8}\left[\frac{3}{4}g_{(2)}(\mu_0)\right]^2 . \tag{3.30}$$

3.4 Summary of results

From the discussions in section 2 and the construction of the effective Lagrangian in ref. [22], we can compile a list of fundamental questions that deserve a phenomenological discussion. For fermions:

(F1) What are the (g_*, M) constraints if DM and the SM fermions are composite: ${}_6\mathcal{F}_\psi^V$?

(F2) What reach in (g_*, M) have DM experiments, if DM is a Goldstino: ${}_8\mathcal{F}_\psi^{(\prime)}$?

(F3) What if the gluons are composite (according to ref. [19]): ${}_8\mathcal{F}_G$?

Moreover it would be interesting to verify the consistency of the assumptions that led to our construction:

(F4) $D = 8$ are small unless a symmetry differentiates them from $D = 6$: ${}_6\mathcal{F}_\psi^V$ vs. ${}_8\mathcal{F}_\psi^V$.

(F5) Chiral symm. breaking operators can be neglected at LHC for light DM: ${}_8\mathcal{F}_G^{\not S}$ vs. ${}_8\mathcal{F}_G$.

(F6) If gluons are composite, can the operators of eq. (2.4) dominate: ${}_6\mathcal{F}_\psi^V$ vs ${}_8\mathcal{F}_\psi^{\rm mono}$?

Similar questions can be asked for scalar DM. In particular we are interested in

(S1) What are the (g_*, M) constraints if DM is a multi-component PNGB and the SM fermions are composite: ${}_6\mathcal{S}_\psi^V$?

(S2) What reach in (g_*, M) have DM experiments, if DM is a PNGB of an abelian SSB pattern: ${}_8\mathcal{S}_G^{S,T}$ and ${}_8\mathcal{S}_\psi^T$?

JHEP11(2016)069

F1 — composite fermions. The case of composite fermions ${}_6\mathcal{F}_\psi^V$ has already been discussed in previous literature (see in particular ref. [23] that uses our same power-counting); we show our results in figure 1. It is interesting that EFT-consistent LHC searches exactly exclude the light-mass region where the RD is correctly reproduced, and where DD experiments have no access (recall also that DD constraints are mostly relevant for the VV chiral structure). This figure also shows in practice the necessity for a strong coupling: constraints consistent with the EFT assumption only exist for a coupling $g_* \gtrsim 2$ [22]. Notice that the particular chiral structure of these higher dimension operators (solid versus dashed lines) has little impact on the constraints away from threshold: this motivated our choice of Weyl basis in the first place.[17] Finally, in this scenario (differently from what we will discuss below) a single interaction dominates at all energies so that the complementarity between LHC, RD and DD constraints, is solid. This is confirmed by the fact that, in this scenario, the effects of $D = 8$ operators is small (question **F4**), as can be seen by comparing the constraints in figure 1 (on a $D = 6$ operator) with those in figure 2 (on a $D = 8$ operator with the same field content): the latter are always poorer, meaning that their effect is smaller.

F2 — Goldstini. The case of Goldstini is novel to our analysis, we will therefore highlight differences w.r.t. the previous case. Non-linearly realized supersymmetry suppresses $D = 6$ (${}_6\mathcal{F}_\psi^V$) w.r.t. $D = 8$ (${}_8\mathcal{F}_\psi^{(\prime)}$) operators; the former are suppressed by $\sim m_\chi^2/M^2$ once explicit SUSY breaking[18] effects that give DM a mass are taken into account.

Beside the poorer collider reach on this scenario (figure 2), the most important aspect of the Goldstino case, concerns DM complementarity. At the LHC, for $E \gg m_\chi$ the $D = 8$ effects, scaling in the amplitude as $\sim g_*^2 E^4/M^4$, dominate over the SUSY breaking $D = 6$ ones, scaling as $\sim g_*^2 m_\chi^2 E^2/M^4$ — see also the left panel of figure 3 for a quantitative analysis of this statement. This is not the case however at the lower energies $E^2 \sim m_\chi^2$ (cf. eq. (3.3)), relevant for the computation of the RD: there the two contributions are comparable. This is exacerbated by the fact that in DM annihilation the $D = 8$ operators are always p-wave suppressed, while the SUSY-breaking $D = 6$ ones are s-wave, and hence enhanced. This implies that the error that we are committing when extracting RD constraints from the $D = 8$ operator, are at least of order 100%. This is key to interpret the results from figure 2 which shows constraints on the single operator ${}_8\mathcal{F}_\psi$ in the Goldstino scenario: the RD band has to be taken as a rough indication only.

Similar arguments apply to DD experiments, whose characteristic energy scale can be as low as the momentum transfer $|\vec{q}| = \sqrt{2 E_{\rm NR} M_{\rm Xe}} \simeq 0.05\,\text{GeV}$, with typical values $E_{\rm NR} = 10\,\text{keV}$, $M_{\rm Xe} = 120\,\text{GeV}$ for a target atom of Xenon. This is particularly visible for the operator ${}_8\mathcal{F}'_\psi$, that receives LHC constraints comparable to ${}_8\mathcal{F}_\psi$, but in DD experiments its energy-dependence extends as low as $E \sim |\vec{q}|$ and makes the effects of this operator

[17] In fact different chiral structures can introduce factors of 2 in the relevant cross sections even at high-E. Such factors of 2 are anyway not taken into account in our generic power-counting and, moreover, we expect that in strongly coupled scenarios different chiral structures are generated at the same time. So, in situations were LHC constraints differ substantially for different chiral structures, we include here only the strongest ones.

[18] In the scenario of ref. [31, 32], $\mathcal{N} = 1$ SUSY is not strictly speaking broken; SUSY breaking effects refer here to explicit departure from the sequestered limit with $\mathcal{N} > 1$ supersymmetries.

JHEP11(2016)069

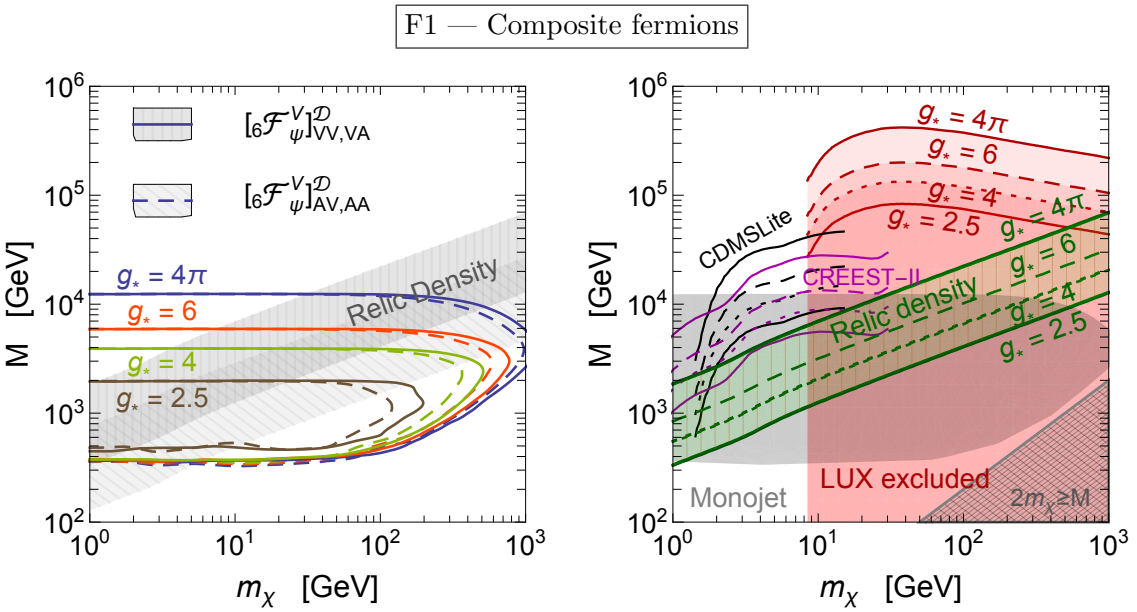

Figure 1. Constraints on DM mass versus new physics scale M for different values of g_* in a model with composite fermions (including fermionic DM), operator ${}_6\mathcal{F}^V_\psi$. LEFT: LHC constraints as colored solid (dashed) lines for the VV and VA (AA and AV) chiral structure; shadows correspond to RD constraints for different couplings and chiral structure, light for AV, AA and dark for VV, VA. RIGHT: constraints from DD and RD for the VV structure (other structures give weaker constraints); shadowed the LHC bounds and hashed the region where $2m_\chi \geq M$ and therefore the EFT description breaks down.

unobservable (see discussion below eq. (3.23)). It is clear that in this situation DD are more likely to see the effects of the SUSY breaking operator $g_*^2 m_\chi^2 ({}_6\mathcal{F}^V_\psi)/M^4$. Of course it is not always the case that DD experiments are irrelevant for $D = 8$ operators. Indeed, in the non-relativistic limit, momentum and mass provide independent energy scales and, while ${}_8\mathcal{F}'_\psi$ is sensitive to the former, ${}_8\mathcal{F}_\psi$ is to the latter. So, with $E \sim m_\chi$ this situation is similar to that of RD discussed above: DD constraints on the effects generated by the SUSY preserving ${}_8\mathcal{F}_\psi$, are comparable to those from the SUSY breaking $g_*^2 m_\chi^2 {}_6\mathcal{F}^V_\psi/M^4$.

In summary, in well-defined scenarios with unsuppressed $D = 8$ and suppressed $D = 6$ effects, DD experiments and the RD are typically sensitive to different effects than collider experiments (either so, or RD and DD experiments receive equivalent contributions from other operators, that are instead suppressed at colliders): the low/high energy complementarity that makes the comparison possible is in this case weak; we nevertheless show the largest constraint you can obtain from DD experiments in figure 2. Given these uncertainties, in addition to those associated with the possibility of a non-standard thermal history, we can conclude that the LHC provides important information on this model with $D = 8$ strong interactions.

F3 — fermion DM with composite gluons. In most BSM models, the transverse polarizations of vector bosons are assumed to be elementary and associated with the SM couplings g, g', g_s. In this case, operators ${}_8\mathcal{F}^{\not{G}}_G$ and ${}_8\mathcal{F}_G$ are always suppressed by α_{em} or

JHEP11(2016)069

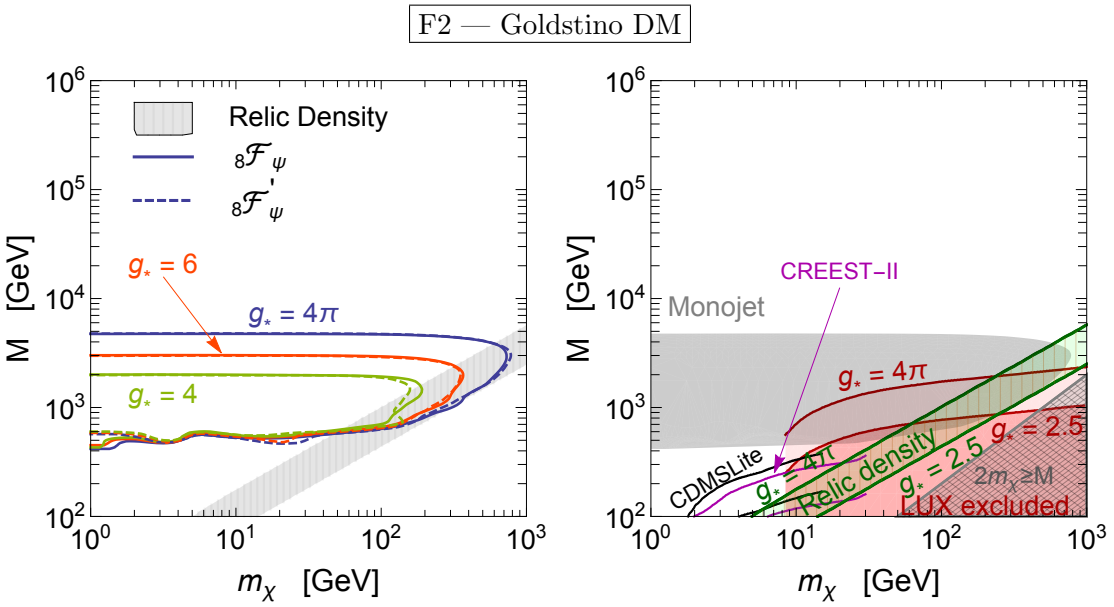

Figure 2. Same as figure 1, but for the $D = 8$ operator ${}_8\mathcal{F}_\psi$ (${}_8\mathcal{F}'_\psi$) in solid (dashed). All constraints apply to Majorana DM, relevant for the Goldstino case.

α_s and their impact for LHC DM searches always negligible. Ref. [19] proposes however a scenario, based on deformed symmetries, where these operators are sizable. The constraints from DM searches on the possibility that DM be strongly coupled to gluons with deformed symmetry, is shown in figure 3.

In this context we take the opportunity to discuss a few consistency aspects of our analysis (questions **F5**, **F6**). First of all, we compare in the right panel of figure 3 the collider constraints from the operators with and without the mass suppression associated with chiral symmetry breaking, ${}_8\mathcal{F}_G^{\not\chi}$ versus ${}_8\mathcal{F}_G$. This clearly shows that for the interesting region with small $m_{\rm DM}$, chiral symmetry breaking operators play a negligible rôle — confirming **F5**.

Secondly, strongly interacting gluons [19] have large multipole interactions (associated with $G^a_{\mu\nu}$) but small monopole interactions (associated with the covariant derivative). In this extreme situation, it is not clear whether emitting an additional jet directly from the new physics vertex (an effect that is captured for instance by the $D = 8$ operator ${}_8\mathcal{F}_\psi^{\rm mono}$), might not have a larger probability than emitting an initial state radiation (ISR) gluon from the quark in ${}_6\mathcal{F}_\psi^V$ — question **F6**. The relative cross sections for $\sigma(pp \to \chi\chi + j)$ scale as

$$\frac{\sigma|_{{}_6\mathcal{F}_\psi^V}}{\sigma|_{{}_8\mathcal{F}_\psi^{\rm mono}}} \sim \frac{g_s^2}{g_*^2}\frac{E^4}{M^4}\,, \tag{3.31}$$

and whether or not it is necessarily larger than unity, depends on the details of the analysis. We perform this comparison in the right panel of figure 3 (dashed versus solid curves), showing that the two are in fact comparable. This exposes a limitation of describing inclusive observables in extreme strongly coupled situations with a parametrization designed for the $2 \to 2$ process $SM + SM \to DM + DM$. In what follows we shall assume that the SM couplings to the strong mediator sector are slightly suppressed w.r.t.

JHEP11(2016)069

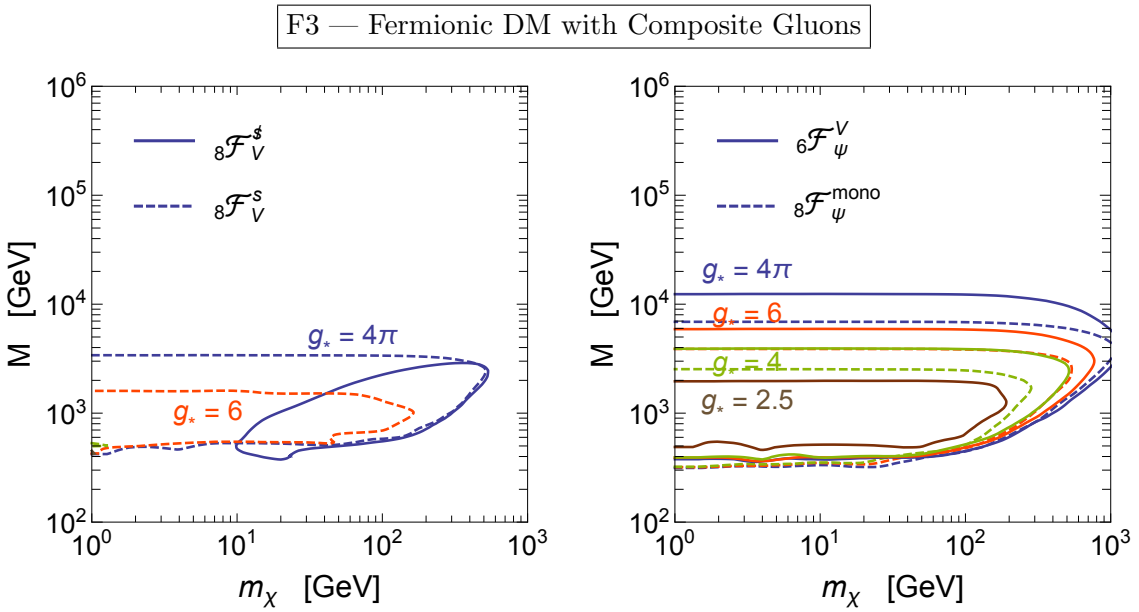

Figure 3. Same labelling as figure 1. LEFT: comparison of constraints from the chirality-breaking, mass-suppressed operator ${}_8\mathcal{F}_G^{\not s}$ (solid) with the unsuppressed ${}_8\mathcal{F}_G$ (dashed). RIGHT: comparison between constraints on ${}_6\mathcal{F}_\psi^V$ (solid), where an additional mono-jets is emitted as ISR, versus constraints on ${}_8\mathcal{F}_\psi^{\rm mono}$ (dashed) where a hard jet is emitted from the new strong interaction directly.

to the DM couplings, a requirement that might also justify the absence of any departure in pure $SM + SM \to SM + SM$ amplitudes in high-momentum distributions. Then the parametrization discussed so far in terms of 4-point amplitudes is consistent.

S1 — complex scalar PNGB DM. In this case the leading interactions between DM and the proton constituents are captured by the $D = 6$ operator ${}_6\mathcal{S}_\psi^V$. The same operator describes well the DM interactions at the energies relevant for computation of the RD and DD. So that the comparison between collider constraints and indications from the RD and DD experiments in figure 4 is solid (notice however that while different chiral structures have equivalent LHC limits, those from DD do depend on the chiral structure).

S2 — real scalar PNGB DM. If the DM is instead associated with a single degree of freedom, as in the case of the abelian SSB U(1) $\to Z_2$, or SO(6)/SO(5), the first strong interactions with (composite) SM fermions arise at $D = 8$: we show the constraints from ${}_8\mathcal{S}_\psi^T$ and ${}_8\mathcal{S}_G^{S,T}$ (for this interaction to be large vectors are also assumed to be composite) in figure 5.

This scenario shares some similarities with the Goldstino case discussed above, but it's interesting to appreciate the differences. In particular in the case that the coupling to gluons dominates, the high energy regime is dominated by ${}_8\mathcal{S}_G^{S,T}$, while at lower energy (for the RD and DD), the symmetry breaking operator ${}_8\mathcal{S}_G^{\not s}$ contributes effects of the same order. More precisely: ${}_8\mathcal{S}_G^S$ has s-wave annihilation like ${}_8\mathcal{S}_G^{\not s}$, but ${}_8\mathcal{S}_G^T$ has only a d-wave annihilation, so that in fact it is subleading to the symmetry breaking effects ${}_8\mathcal{S}_G^{\not s}$ during freeze-out. If instead the couplings to fermions are more important, then we have an interesting twist in the

JHEP11(2016)069

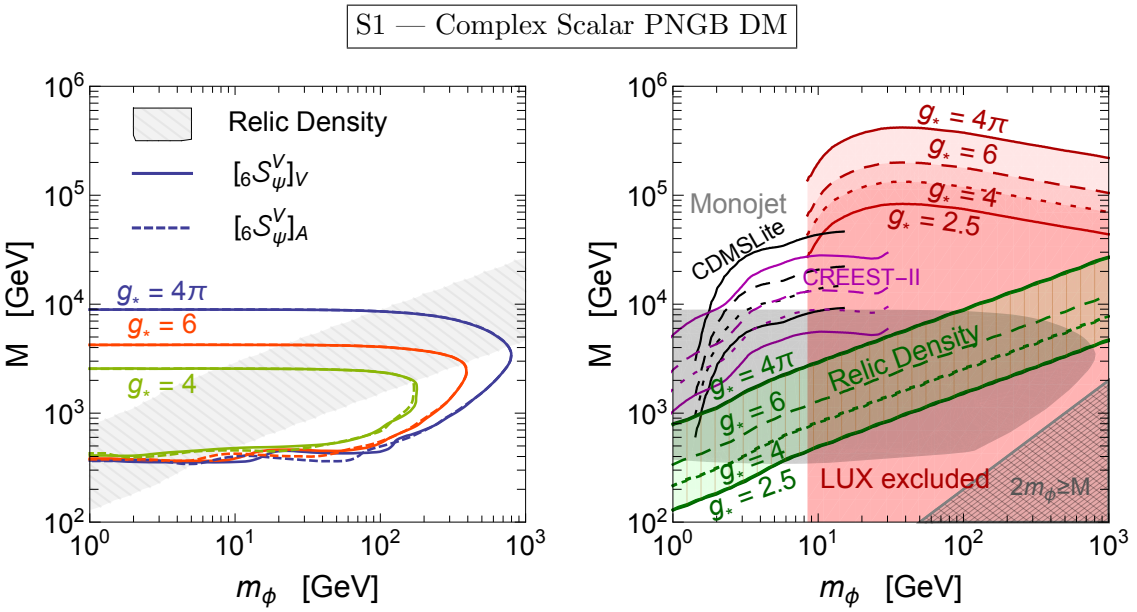

Figure 4. Operator $[{}_6\mathcal{S}^V_\psi]_V([{}_6\mathcal{S}^V_\psi]_A)$ in solid (dashed) with ϕ a complex scalar — labelling as in figure 1, DD constraints only for the vector structure $[{}_6\mathcal{S}^V_\psi]_V$.

U(1)/$\mathcal{Z}_2$ case. Here the effects that break the non-linearly realized U(1) symmetry are captured by ${}_6\mathcal{S}^{\not\phi}_\psi$, which accidentally is further suppressed by the small SM Yukawas. For this reason, differently from the Goldstino case, symmetry breaking effects do not play an important rôle at freeze-out and the computation of the RD based on ${}_8\mathcal{S}^T_\psi$ are to be taken more seriously; for DD, on the other hand, quark-mass suppressed effects in the nucleon matrix element are enhanced and eventually appear proportional to $m_N \approx 1\,\text{GeV}$, introducing an error $\sim m_N/m_\phi$ in the DD constraint based on ${}_8\mathcal{S}^T_\psi$ only. In the SO(6)/SO(5) case (see the third bullets of page 6 or the table in [22]), the operators ${}_6\mathcal{S}^{\not\phi}_\psi$ and ${}_6\mathcal{S}^S_H$ are not suppressed by the mass and do play a rôle in the computation of RD, as discussed in detail in [43].

4 Conclusions and outlook

We have studied scenarios for LHC DM searches based on underlying strongly coupled dynamics. In these situations, the difficulty of performing perturbative calculations imply that an EFT describing the low-energy degrees of freedom is in fact necessary. Moreover, despite the large separation of scales $E^{LHC} \ll M$ required for the EFT to be predictive, these scenarios can produce sizable effects (enhanced by the strong coupling), visible in LHC searches based on missing energy. The crucial ingredient that guarantees the existence of a weakly coupled SM at low energy, and the realization of the WIMP miracle, compatibly with an underlying strong coupling, is *approximate global symmetry*. We have identified 4 unique scenarios where light composite states (recognized with DM) can emerge from the strong dynamics that match to the EFT we consider: scalar PNGB of a non-linearly realized abelian (**S2**) or non-abelian (**S1**) symmetry, composite fermions with chiral symmetry (**F1**)

JHEP11(2016)069

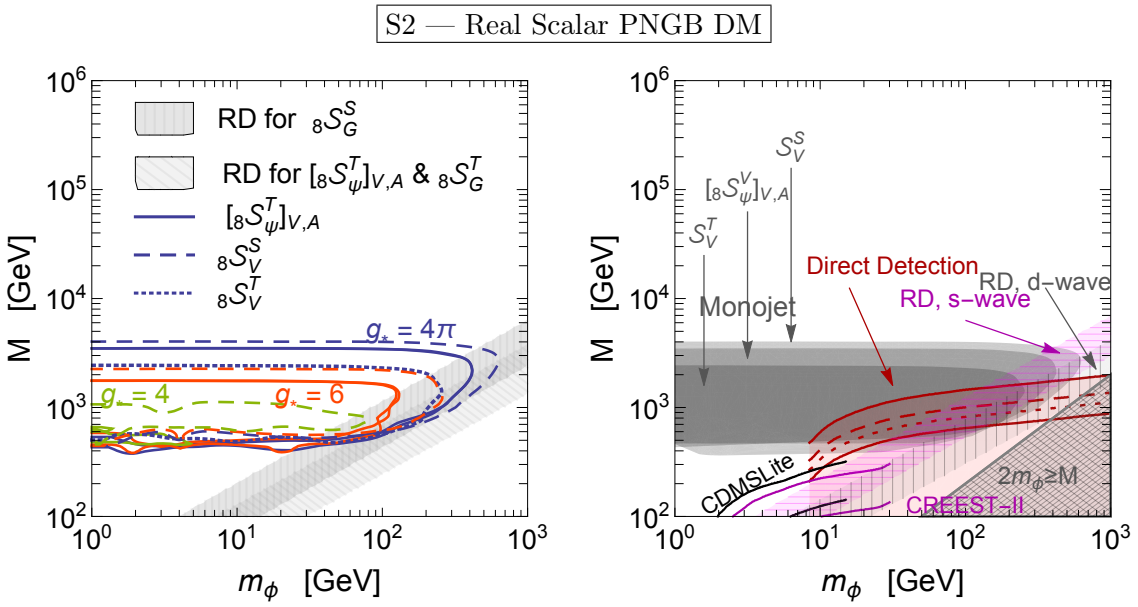

Figure 5. Constraints on various $D = 8$ operators for a real scalar PNGB. LEFT: LHC constraints. RIGHT: for the RD operator ${}_8\mathcal{S}_G^S({}_8\mathcal{S}_G^T)$ annihilate in s-(d-)wave; DD bounds are universal for all operators, except $[{}_8\mathcal{S}_\psi^V]_A$. Color code as previous figures.

and Goldstini of non-linearly realized supersymmetry, spontaneously broken by strong dynamics (**F2**).

Cases **S2** and **F2** are particularly interesting and novel to our discussion, since the associated operators are characterized by higher derivatives ($D = 8$), while lower-dimension effects are suppressed by powers of the small DM mass. At the LHC, the large energy $E \gg m_{\rm DM}$ implies that mass suppressed effects are subdominant. For computations of the RD, on the other hand, $E \approx m_{\rm DM}$, so that symmetry breaking and symmetry preserving effects turn out to be often comparable: DM complementarity, thought as a comparison of different constraints individually for each operator, is here lost, since different effects dominate at different energies. This is even more relevant when constraints from DD are included. Depending on the chiral structure of a given operator, its contribution to the amplitudes relevant for DD might be proportional to the momentum transfer, and hence suppressed. In other instances, this contribution might scale like the DM rest mass, and arguments similar to RD apply for DD. Our discussion shows the limits of comparing experimental constraints from widely separated regimes on individual operators, without a solid BSM perspective. The LHC reach on these models is represented in figures 5 and 2, where constraints from RD and DD have to be taken as a rough indication only: symmetry breaking effects introduce an $O(1)$ uncertainty. Given this uncertainty and our ignorance about the thermal history of the universe, we conclude that the LHC is providing important information on these models, constraining an interesting region of parameter space associated with very large couplings.

Cases **S1** and **F1** are instead closer to what has been studied in previous literature, in terms of their effective Lagrangian. Yet, the power counting that we have introduced allows to relate specific UV assumptions with the size of coefficients of EFT operators and

JHEP11(2016)069

understand what effects can be expected large. In particular, sizable couplings to gluons are only possible if these have strong multipolar interactions, following the construction of ref. [19]. Moreover, it highlights the necessity of strong coupling, as can be seen in most of our figures, where constraints consistent with the EFT description exist only for very large couplings (see also [22]).[19] In these cases the comparison of LHC mono-jet searches with DD and RD experiments is rather solid, since symmetry breaking effects are typically further suppressed by small Yuakawa couplings. We show the results in figures 4 and 1. First of all, our analysis reveals the interesting fact that even inherently strongly coupled DM can reproduce the correct RD, as long as an approximate symmetry forbids the lower-dimension interactions.[20] Secondly, it shows that LHC experiments are pounding the very region of parameter space where the RD is correctly reproduced.

In general, our scenario (in particular the novel **S2** and **F2**) provide an interesting modeling of missing transverse energy processes for the LHC (similar in that sense to the spirit of simplified models), which is inspired by an explicit UV realization but captured by a simple bottom-up EFT parametrization.

Natural extensions of our study, which we plan to entertain in the near future, include studies of mono-W [88], mono-Z [89], mono-h [90] and mono-γ [91] processes with the EFT classification proposed in [22] and discussed in section 2. In particular it is already interesting to recall that the operators $\phi^\dagger \overset{\leftrightarrow}{\partial}_\mu \phi \, H^\dagger \overset{\leftrightarrow}{D^\mu} H$ and $\chi^\dagger \bar{\sigma}^\mu \chi H^\dagger \overset{\leftrightarrow}{D}_\mu H$ have been discarded from our analysis, as they violate custodial symmetry: this represent another instance where the hierarchy of operators that is traditionally assumed (associated uniquely to the $1/M$ expansion) is compromised in the presence of approximate symmetries. Another avenue that we intend to pursue stems from arguments based on the analyticity of scattering amplitudes, together with crossing symmetry and unitarity, that allow to extract some information, based on prime principles, about the coefficients of operators with a particularly soft IR behaviour. In our case this takes the form of positivity constraints on some of the coefficients of the EFT operators; from a practical point of view this corresponds to a theoretical prior in which to perform the statistical analysis.

Acknowledgments

We are mostly indebted with Rakhi Mahbubani for her help in the collider analysis and her comments or suggestions (including the title!). We also acknowledge important conversations with Mikael Chala, Roberto Contino, Felix Kahlhoefer, Matthew McCullough, Alex Pomarol, Davide Racco, Riccardo Rattazzi, Andrea Wulzer.

[19] Notice that in practice in the limit $g_* \simeq 4\pi$, the cutoff $\sqrt{s} < M$ is equivalent to the constraint obtained using partial wave unitarity arguments [85, 86]; our construction, however, provides a well-defined hypothesis testing and a consistent physical picture of the meaning of unitarity breakdown.

[20] On the same lines ref. [87] suppressed $2 \to 2$ interactions in favor of $2 \to 3$ which also allows a strong coupling to be compatible with the observed RD.

JHEP11(2016)069

A Notation and conventions

This appendix is dedicated to expanding on our notation in terms of Weyl spinors and comparing with previous literature. We also include details relative to the computation of RD and direct detection cross sections that have been neglected in the main text.

A.1 Fermions in two-component notation

The building blocks of the Dirac Lagrangian $\mathcal{L}_\Psi = \bar{\Psi} i\gamma^\mu(\partial_\mu\Psi) - m_\Psi\bar{\Psi}\Psi$ in two-component spinor notation are

$$\Psi = \begin{pmatrix} \xi_\alpha \\ \eta^{\dagger\dot{\alpha}} \end{pmatrix}, \quad \bar{\Psi} = \begin{pmatrix} \eta^\alpha & \xi^\dagger_{\dot{\alpha}} \end{pmatrix}, \quad \gamma_\mu = \begin{pmatrix} 0 & (\sigma_\mu)_{\alpha\dot{\beta}} \\ (\bar{\sigma}_\mu)^{\dot{\alpha}\beta} & 0 \end{pmatrix}. \tag{A.1}$$

where the two Weyl spinors ξ_α and $\eta^{\dagger\dot{\alpha}}$ transform under the $(1/2, 0)$ and $(0, 1/2)$ representations of the Lorentz group $\mathrm{SO}(1,3) \simeq \mathrm{SL}(2,\mathbb{C})$. The Pauli matrices $\sigma_{i=1,2,3}$ define $\sigma^\mu = (\mathbb{1}_2, \vec{\sigma})$ and $\bar{\sigma}^\mu = (\mathbb{1}_2, -\vec{\sigma})$, so that

$$\mathcal{L}_\Psi = \xi^\dagger i\bar{\sigma}^\mu(\partial_\mu\xi) + \eta^\dagger i\bar{\sigma}^\mu(\partial_\mu\eta) - m_\Psi(\xi\eta + \eta^\dagger\xi^\dagger), \tag{A.2}$$

with Lorentz-invariant spinor contractions $\xi\eta \equiv \xi^\alpha\eta_\alpha = \xi^\alpha\epsilon_{\alpha\beta}\eta^\beta = -\eta^\beta\epsilon_{\alpha\beta}\xi^\alpha = \eta^\beta\epsilon_{\beta\alpha}\xi^\alpha = \eta^\beta\xi_\beta = \eta\xi$. For two four-component spinors $\Psi_{1,2}$, the relevant fermion bilinears in four- and two-component notation are

$$\bar{\Psi}_1 P_L \Psi_2 = \eta_1\xi_2, \quad \bar{\Psi}_1 P_R \Psi_2 = \xi_1^\dagger\eta_2^\dagger, \quad \bar{\Psi}_1\gamma^\mu P_L\Psi_2 = \xi_1^\dagger\bar{\sigma}_\mu\xi_2, \quad \bar{\Psi}_1\gamma_\mu P_R\Psi_2 = -\eta_2^\dagger\bar{\sigma}_\mu\eta_2 \tag{A.3}$$

A.2 Fermionic DM: effective operators in matrix form

The comparison between Weyl and Dirac notation is captured by the definition

$$\textbf{Weyl: } \chi = (\xi_1, \eta_1) \quad \psi = (\xi_2, \eta_2) \quad \textbf{Dirac: } \boldsymbol{\chi} = \begin{pmatrix} \xi_{1\alpha} \\ \eta_1^{\dagger\dot{\alpha}} \end{pmatrix} \quad \Psi = \begin{pmatrix} \xi_{2\alpha} \\ \eta_2^{\dagger\dot{\alpha}} \end{pmatrix}, \tag{A.4}$$

where in our notation, the two components of ξ and ψ are summed as elements of a vector, thinking of the Wilson coefficients as matrices, while in Dirac notation they are grouped into a 4-component vector. This will become clearer in the case by case analysis that follows.

$\boxed{\boldsymbol{6\mathcal{F}_\psi^V}}$ There are four possible $D = 6$ operators coupling the two fermions

$$\begin{aligned} c_\psi[\xi^\dagger\bar{\sigma}^\mu\xi][\psi^\dagger\bar{\sigma}^\mu\psi] \equiv & \begin{pmatrix} \xi_1^\dagger\bar{\sigma}^\mu\xi_1 & \eta_1^\dagger\bar{\sigma}^\mu\eta_1 \end{pmatrix} \underbrace{\begin{pmatrix} c_\psi^{11} & c_\psi^{12} \\ c_\psi^{21} & c_\psi^{22} \end{pmatrix}}_{c_\psi\in\mathbb{R}} \begin{pmatrix} \xi_2^\dagger\bar{\sigma}_\mu\xi_2 \\ \eta_2^\dagger\bar{\sigma}_\mu\eta_2 \end{pmatrix} \\ = & \, c_{VV}^\psi\left[\bar{\boldsymbol{\chi}}\gamma^\mu\boldsymbol{\chi}\right]\left[\bar{\Psi}\gamma_\mu\Psi\right] + c_{VA}^\psi\left[\bar{\boldsymbol{\chi}}\gamma^\mu\boldsymbol{\chi}\right]\left[\bar{\Psi}\gamma_\mu\gamma^5\Psi\right] \\ & + c_{AV}^\psi\left[\bar{\boldsymbol{\chi}}\gamma^\mu\gamma^5\boldsymbol{\chi}\right]\left[\bar{\Psi}\gamma_\mu\Psi\right] + c_{AA}^\psi\left[\bar{\boldsymbol{\chi}}\gamma^\mu\gamma^5\boldsymbol{\chi}\right]\left[\bar{\Psi}\gamma_\mu\gamma^5\Psi\right], \end{aligned} \tag{A.5}$$

where we defined the four linear independent combinations

$$c_{VV}^{\psi} \equiv \frac{1}{4}\left(c_{\psi}^{11} - c_{\psi}^{12} - c_{\psi}^{21} + c_{\psi}^{22}\right) , \qquad c_{VA}^{\psi} \equiv \frac{1}{4}\left(-c_{\psi}^{11} - c_{\psi}^{12} + c_{\psi}^{21} + c_{\psi}^{22}\right) , \tag{A.6}$$

$$c_{AV}^{\psi} \equiv \frac{1}{4}\left(-c_{\psi}^{11} + c_{\psi}^{12} - c_{\psi}^{21} + c_{\psi}^{22}\right) , \qquad c_{AA}^{\psi} \equiv \frac{1}{4}\left(c_{\psi}^{11} + c_{\psi}^{12} + c_{\psi}^{21} + c_{\psi}^{22}\right) . \tag{A.7}$$

Eq. (A.5) shows the clear advantage of our notation, since one matrix structure embodies four different chiral operators. From the CP transformation properties

$$CP\left\{\bar{\Psi}_i \Gamma^{\mu} \Psi_i\right\} = (-1)(-1)^{\mu} \bar{\Psi}_i \Gamma^{\mu} \Psi_i \, , \tag{A.8}$$

with both $\Gamma^{\mu} = \gamma^{\mu}, \gamma^{\mu}\gamma^5$ follows that the four operators in eq. (A.5) are CP-invariant. Finally, note that if $\boldsymbol{\chi}$ is a Majorana fermion, $\boldsymbol{\chi}^C = \boldsymbol{\chi}$, the vector bilinear vanishes since $\bar{\boldsymbol{\chi}}\gamma^{\mu}\boldsymbol{\chi} = -\bar{\boldsymbol{\chi}}\gamma^{\mu}\boldsymbol{\chi}$, and the only surviving operators are c_{AV} and c_{AA}. In the following we refer to the four operators with the notation $[{}_6\mathcal{F}_{\psi}^{V}]^{\mathcal{D},\mathcal{M}}_{AV,VV,VA,AA}$, in which the additional lower index refers to the chiral structure of the corresponding operator (first letter for the DM current, second for the SM current). The upper index refers to the Majorana ($\mathcal{M}$) or Dirac ($\mathcal{D}$) nature of the DM particle.

Relic density. We complement the information given in the text with an explicit calculation of the annihilation cross section for massive fermions; we find

$$\sigma v_{\rm rel}|_{[{}_6\mathcal{F}_{\psi}^{V}]^{\mathcal{D}}_{AV}} = \frac{c_{AV}^{\psi\,2} g_*^4}{M^4}\left[\frac{m_\chi^2\sqrt{1-x_\psi^2}(2+x_\psi^2)v_{\rm rel}^2}{4\pi} + \mathcal{O}(v_{\rm rel}^4)\right] , \tag{A.9}$$

$$\sigma v_{\rm rel}|_{[{}_6\mathcal{F}_{\psi}^{V}]^{\mathcal{D}}_{VV}} = \frac{c_{VV}^{\psi\,2} g_*^4}{M^4}\left[\underbrace{\frac{3m_\chi^2\sqrt{1-x_\psi^2}(2+x_\psi^2)}{2\pi}}_{\text{unsuppressed s-wave}} + \frac{m_\chi^2(8-4x_\psi^2+5x_\psi^4)v_{\rm rel}^2}{16\pi\sqrt{1-x_\psi^2}} + \mathcal{O}(v_{\rm rel}^4)\right] , \tag{A.10}$$

$$\sigma v_{\rm rel}|_{[{}_6\mathcal{F}_{\psi}^{V}]^{\mathcal{D}}_{VA}} = \frac{c_{VA}^{\psi\,2} g_*^4}{M^4}\left[\underbrace{\frac{3m_\chi^2(1-x_\psi^2)^{3/2}}{\pi}}_{\text{unsuppressed s-wave}} + \frac{m_\chi^2\sqrt{1-x_\psi^2}(4+5x_\psi^2)v_{\rm rel}^2}{8\pi} + \mathcal{O}(v_{\rm rel}^4)\right] , \tag{A.11}$$

$$\sigma v_{\rm rel}|_{[{}_6\mathcal{F}_{\psi}^{V}]^{\mathcal{D}}_{AA}} = \frac{c_{AA}^{\psi\,2} g_*^4}{M^4}\left[\underbrace{\frac{3m_\psi^2}{2\pi}\sqrt{1-x_\psi^2}}_{\text{suppressed s-wave}} + \frac{m_\chi^2(8-22x_\psi^2+17x_\psi^4)v_{\rm rel}^2}{16\pi\sqrt{1-x_\psi^2}} + \mathcal{O}(v_{\rm rel}^4)\right] , \tag{A.12}$$

with $x_\psi \equiv m_\psi/m_\chi$. This confirms our arguments based on conserved chiral symmetry, given in section 3.2. Eqs. (A.9)–(A.12) are valid for a Dirac DM particle; for Majorana DM, eqs. (A.10)–(A.11) are equal to zero while the annihilation cross sections corresponding to the operators $[{}_6\mathcal{F}_{\psi}^{V}]_{AV}$ and $[{}_6\mathcal{F}_{\psi}^{V}]_{AA}$ must be multiplied by a factor of 4 since the number of diagrams in the scattering amplitude — fermions being equivalent to anti-fermions — doubles.

JHEP11(2016)069

Direct detection. At the nucleon level, the amplitudes for the DM-nucleon scattering in the non-relativistic limit are

$$\mathcal{M}_N|_{[{}_6\mathcal{F}^V_\psi]_{AV}} = \frac{8c_{AV}g_*^2 m_\chi}{M^2}\left[m_N\vec{s}_\chi\cdot\vec{v}^\perp + i\vec{s}_\chi\cdot(\vec{s}_N\times\vec{q})\right]\times\begin{cases}2c^u_{AV}+c^d_{AV} & (N=p)\\ c^u_{AV}+2c^d_{AV} & (N=n)\end{cases} \tag{A.13}$$

$$\mathcal{M}_N|_{[{}_6\mathcal{F}^V_\psi]_{VV}} = \frac{4g_*^2 m_\chi m_N}{M^2}\times\begin{cases}2c^u_{VV}+c^d_{VV} & (N=p)\\ c^u_{VV}+2c^d_{VV} & (N=n)\end{cases} \tag{A.14}$$

$$\mathcal{M}_N|_{[{}_6\mathcal{F}^V_\psi]_{VA}} = \frac{8g_*^2 m_N}{M^2}\left[-m_\chi\vec{s}_N\cdot\vec{v}^\perp + i\vec{s}_\chi\cdot(\vec{s}_N\times\vec{q})\right]\left(\sum_{\psi=u,d,s}c^\psi_{VA}\Delta^{(N)}_\psi\right), \tag{A.15}$$

$$\mathcal{M}_N|_{[{}_6\mathcal{F}^V_\psi]_{AA}} = -\frac{16g_*^2 m_\chi m_N}{M^2}(\vec{s}_\chi\cdot\vec{s}_N)\left(\sum_{\psi=u,d,s}c^\psi_{AA}\Delta^{(N)}_\psi\right), \tag{A.16}$$

where the coefficients $\Delta^{(N)}_\psi$, implicitly defined through the nuclear matrix element $2\Delta^{(N)}_\psi s^\mu = \langle N|\bar{\psi}\gamma^\mu\gamma^5\psi|N\rangle$ parametrize the quark spin content of the nucleon N (s^μ is the spin nucleon four-vector). We refer to [82] for the corresponding numerical values. As discussed in the text, the operator $[{}_6\mathcal{F}^V_\psi]^{\mathcal{D}}_{VV}$ generates a non-vanishing DM-nucleon spin-independent elastic cross section that is not suppressed by small DM velocity or momentum transfer, while $\mathcal{M}_N|_{[{}_6\mathcal{F}^V_\psi]_{VA}}$ is certainly poorly constrained since it leads to a spin-dependent cross section suppressed also by $\vec{v}^\perp$ or $\vec{q}$. The amplitude $\mathcal{M}_N|_{[{}_6\mathcal{F}^V_\psi]_{AV}}$, on the contrary, is characterized by a spin-independent contribution suppressed by $\vec{v}^\perp$ only. Given the remarkable constraining power of DD experiments in the presence of a spin-independent cross section, it is worth studying this contribution in more detail (this has been ignored in the main text since it is always subleading to VV, when both are present). This is shown in the left panel of figure 6, in which the region shaded in blue reproduces the observed RD (for different values of g_*, see caption) while DD bounds (from [76], at 90 % C.L.) correspond to lines in red (for each g_*, the region below the corresponding red line is excluded). Finally, the amplitude $\mathcal{M}_N|_{[{}_6\mathcal{F}^V_\psi]_{AA}}$ leads to a spin-dependent cross section that is not suppressed neither by $\vec{v}^\perp$ nor $\vec{q}$. The LUX experiment set in [77] the strongest bound on spin-dependent DM-neutron[21] cross section, and we use this result, at 90 % C.L., to constrain the operator $[{}_6\mathcal{F}^V_\psi]_{AA}$. We show the corresponding exclusion regions in the right panel of figure 6 (red lines, see caption). As far as the DM-proton spin dependent cross section is concerned, strong constraints were obtained by the PICO-2L [93], Super-Kamiokande [94] and IceCube [95] experiments. The former is a bubble chamber experiment while Super-Kamiokande and IceCube are neutrino telescopes that can observe neutrinos originating from annihilation of DM captured in the Sun. For comparison, in figure 6 (black, magenta and green lines, see caption) we show the exclusion regions obtained considering the results of the PICO-2L, Super-Kamiokande and IceCube

[21] DM is coupled to the net spin of a nucleus, generated by its unpaired nucleon. For a Xenon detector, constraints on DM-neutron spin dependent cross section are stronger since there are two naturally occurring Xenon isotopes with an odd number of neutrons, ^{129}Xe and ^{131}Xe.

JHEP11(2016)069

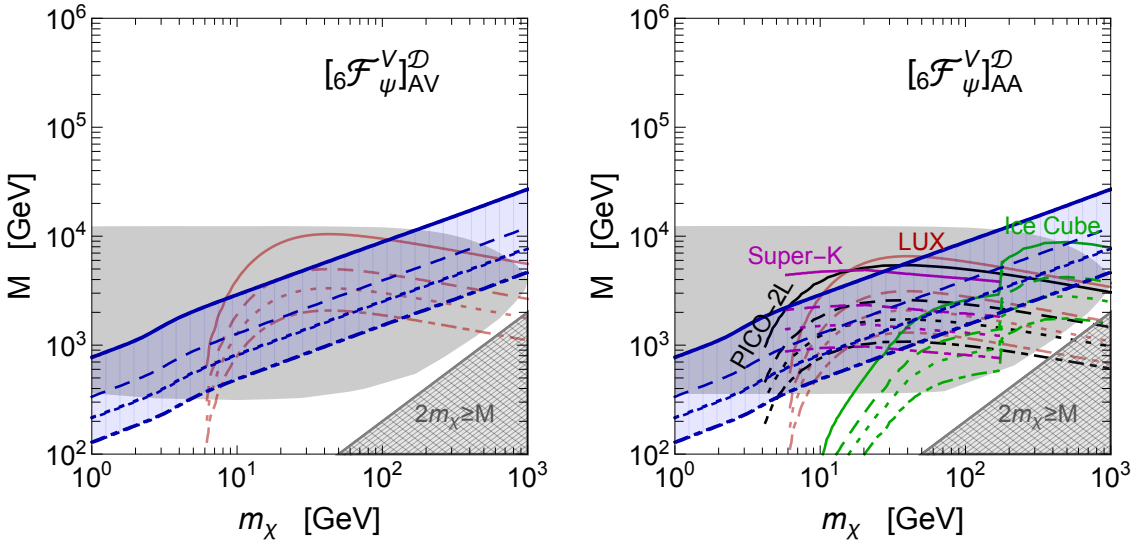

Figure 6. Interplay between LHC, RD, and DD for the operator $[{}_6\mathcal{F}^V_\psi]^{\mathcal{D}}_{AV}$ (left panel) and $[{}_6\mathcal{F}^V_\psi]^{\mathcal{D}}_{VV}$ (right panel). The region shaded in blue reproduces the observed RD while the red lines correspond to DD bounds at 90 % C.L. (left panel: LUX experiment [76], spin-independent DM-nucleon cross section; right panel, red lines (black, magenta, and green lines, respectively): LUX experiment [77] (PICO-2L [93], Super-Kamiokande [94] and IceCube [95] experiments), spin-dependent DM-neutron (DM-proton) cross section). Different lines correspond to different values of strong coupling: $g_* = 4\pi$ (solid), 6 (dashed), 4 (dotted), 2.5 (dot-dashed). The region shaded in gray is excluded by LHC mono-jet searches.

experiments. Notice that Super-Kamiokande and IceCube limits depend on the specific DM annihilation channels. For the Super-Kamiokande results a 100% branching fraction into $b\bar{b}$ has been assumed, whereas in the case of IceCube the full mass dependence of the branching fraction was retained. Notice in particular the opening of the $t\bar{t}$ annihilation channel at $m_\chi = m_t$. Compared to figure 1, DD bounds are much weaker but they still place meaningful constraints on the parameter space in the presence of a strong coupling. However, LHC mono-jet searches set the strongest constraints in the region favored by the observed relic abundance. Figure 6 strengthens the importance of complementarity between LHC, RD and DD constraints for the effective operator ${}_6\mathcal{F}^V_\psi$.

${}_8\mathcal{F}^V_\psi$ We recast this operator in matrix form as

$$C_\psi \Big[\chi^\dagger \bar{\sigma}^\mu (\partial^\nu \chi)\Big]\Big[\psi^\dagger \bar{\sigma}_\mu (\partial_\nu \psi)\Big] \equiv \Big(\xi_1^\dagger \bar{\sigma}^\mu (\partial^\nu \xi_1)\ \eta_1^\dagger \bar{\sigma}^\mu (\partial^\nu \eta_1)\Big) \underbrace{\begin{pmatrix} C_\psi^{11} & C_\psi^{12} \\ C_\psi^{21} & C_\psi^{22} \end{pmatrix}}_{C_\psi \in \mathbb{C}} \begin{pmatrix} \xi_2^\dagger \bar{\sigma}_\mu (\partial_\nu \xi_2) \\ \eta_2^\dagger \bar{\sigma}_\mu (\partial_\nu \eta_2) \end{pmatrix} + h.c.$$

$$= C_{VV}\,[\bar{\boldsymbol{\chi}}\gamma^\mu(\partial^\nu \boldsymbol{\chi})]\,[\bar{\Psi}\gamma_\mu(\partial_\nu \Psi)] + C_{VA}\,[\bar{\boldsymbol{\chi}}\gamma^\mu(\partial^\nu \boldsymbol{\chi})]\,[\bar{\Psi}\gamma_\mu\gamma^5(\partial_\nu \Psi)]$$
$$+ C_{AV}\,[\bar{\boldsymbol{\chi}}\gamma^\mu\gamma^5(\partial^\nu \boldsymbol{\chi})]\,[\bar{\Psi}\gamma_\mu(\partial_\nu \Psi)] + C_{AA}\,[\bar{\boldsymbol{\chi}}\gamma^\mu\gamma^5(\partial^\nu \boldsymbol{\chi})]\,[\bar{\Psi}\gamma_\mu\gamma^5(\partial_\nu \Psi)] + h.c.\,, \quad \text{(A.17)}$$

JHEP11(2016)069

where the coefficients are defined as in eqs. (A.6)–(A.7) with $c \to C$ (with the difference that now we are dealing with complex numbers).

Let us now assume that $\boldsymbol{\chi}$ is a Majorana fermion as for Goldstino DM, with $\boldsymbol{\chi}^C = \boldsymbol{\chi}$. For a Majorana fermion we have[22] $\bar{\boldsymbol{\chi}}\gamma^\mu\gamma^5(\partial^\nu\boldsymbol{\chi}) = (\partial^\nu\bar{\boldsymbol{\chi}})\gamma^\mu\gamma^5\boldsymbol{\chi}$ and $\bar{\boldsymbol{\chi}}\gamma^\mu(\partial^\nu\boldsymbol{\chi}) = -(\partial^\nu\bar{\boldsymbol{\chi}})\gamma^\mu\boldsymbol{\chi}$. Separating real and imaginary part in $C_{ij} \equiv C_{ij}^{\mathbb{R}} + iC_{ij}^{\mathbb{I}\gtrdot}$, and using that

$$CP\left\{\bar{\boldsymbol{\chi}}\gamma^\mu(\partial^\nu\boldsymbol{\chi})\right\} = (-1)^\mu(-1)^\nu\bar{\boldsymbol{\chi}}\gamma^\mu(\partial^\nu\boldsymbol{\chi})\,, \tag{A.19}$$

$$CP\left\{\bar{\boldsymbol{\chi}}\gamma^\mu\gamma^5(\partial^\nu\boldsymbol{\chi})\right\} = (-1)(-1)^\mu(-1)^\nu\bar{\boldsymbol{\chi}}\gamma^\mu\gamma^5(\partial^\nu\boldsymbol{\chi})\,, \tag{A.20}$$

$$CP\left\{\bar{\Psi}\Gamma^\mu(\partial^\nu\Psi) \pm (\partial^\nu\bar{\Psi})\Gamma^\mu\Psi\right\} = (\mp1)(-1)^\mu(-1)^\nu[\bar{\Psi}\Gamma^\mu(\partial^\nu\Psi) \pm (\partial^\nu\bar{\Psi})\Gamma^\mu\Psi]\,, \tag{A.21}$$

with both $\Gamma^\mu = \gamma^\mu, \gamma^\mu\gamma^5$, we end up with the following interactions

$$\begin{aligned}
&C_{VV}^{\mathbb{R}}[\bar{\boldsymbol{\chi}}\gamma^\mu(\partial^\nu\boldsymbol{\chi})] \times \left[\bar{\Psi}\gamma_\mu(\partial_\nu\Psi) - (\partial_\nu\bar{\Psi})\gamma_\mu\Psi\right] && \text{CP-preserving}\\
&iC_{VV}^{\mathbb{I}\gtrdot}[\bar{\boldsymbol{\chi}}\gamma^\mu(\partial^\nu\boldsymbol{\chi})] \times \left[\bar{\Psi}\gamma_\mu(\partial_\nu\Psi) + (\partial_\nu\bar{\Psi})\gamma_\mu\Psi\right] && \text{CP-violating}\\
&C_{VA}^{\mathbb{R}}[\bar{\boldsymbol{\chi}}\gamma^\mu(\partial^\nu\boldsymbol{\chi})] \times \left[\bar{\Psi}\gamma_\mu\gamma^5(\partial_\nu\Psi) - (\partial_\nu\bar{\Psi})\gamma_\mu\gamma^5\Psi\right] && \text{CP-preserving}\\
&iC_{VA}^{\mathbb{I}\gtrdot}[\bar{\boldsymbol{\chi}}\gamma^\mu(\partial^\nu\boldsymbol{\chi})] \times \left[\bar{\Psi}\gamma_\mu\gamma^5(\partial_\nu\Psi) + (\partial_\nu\bar{\Psi})\gamma_\mu\gamma^5\Psi\right] && \text{CP-violating}\\
&C_{AV}^{\mathbb{R}}[\bar{\boldsymbol{\chi}}\gamma^\mu\gamma^5(\partial^\nu\boldsymbol{\chi})] \times \left[\bar{\Psi}\gamma_\mu(\partial_\nu\Psi) + (\partial_\nu\bar{\Psi})\gamma_\mu\Psi\right] && \text{CP-preserving}\\
&iC_{AV}^{\mathbb{I}\gtrdot}[\bar{\boldsymbol{\chi}}\gamma^\mu\gamma^5(\partial^\nu\boldsymbol{\chi})] \times \left[\bar{\Psi}\gamma_\mu(\partial_\nu\Psi) - (\partial_\nu\bar{\Psi})\gamma_\mu\Psi\right] && \text{CP-violating}\\
&C_{AA}^{\mathbb{R}}[\bar{\boldsymbol{\chi}}\gamma^\mu\gamma^5(\partial^\nu\boldsymbol{\chi})] \times \left[\bar{\Psi}\gamma_\mu\gamma^5(\partial_\nu\Psi) + (\partial_\nu\bar{\Psi})\gamma_\mu\gamma^5\Psi\right] && \text{CP-preserving}\\
&iC_{AA}^{\mathbb{I}\gtrdot}[\bar{\boldsymbol{\chi}}\gamma^\mu\gamma^5(\partial^\nu\boldsymbol{\chi})] \times \left[\bar{\Psi}\gamma_\mu\gamma^5(\partial_\nu\Psi) - (\partial_\nu\bar{\Psi})\gamma_\mu\gamma^5\Psi\right] && \text{CP-violating}
\end{aligned} \tag{A.22}$$

We assume CP as a fundamental symmetry, then

$$\mathbb{I}\gtrdot \begin{pmatrix} C_\psi^{11} & C_\psi^{12} \\ C_\psi^{21} & C_\psi^{22} \end{pmatrix} = 0\ . \tag{A.23}$$

In the text we assume coefficients to be real.

Relic density. Goldstino annihilation cannot proceed via s-wave. In the initial state a system of two Majorana particles with $L = 0$ is forced to stay in a state with total spin $S = 0$ (since $C = (-1)^{L+S} \stackrel{!}{=} 1$). As a consequence, $J = 0$ considering s-wave annihilation. However, the tensor current on the SM side has $J = 2$, thus forcing the s-wave to vanish to conserve total angular momentum. The same argument shows that p-wave annihilation is allowed since two Majorana particles with total orbital angular momentum $L = 1$ are forced to stay in a state with total spin $S = 1$ (and hence $J = 2$ is an allowed eigenvalue). In the massless limit for the final state quarks, we find eq. (3.12).

[22] From the definition of charge conjugation we have $\boldsymbol{\chi}^C = \mathcal{C}\bar{\boldsymbol{\chi}}^T$, $\bar{\boldsymbol{\chi}}^C = \boldsymbol{\chi}^T\mathcal{C}$, with $\mathcal{C} \equiv i\gamma^0\gamma^2$. As a consequence we write

$$\begin{aligned}
\bar{\boldsymbol{\chi}}\gamma^\mu\gamma^5(\partial^\nu\boldsymbol{\chi}) &= \bar{\boldsymbol{\chi}}^C\gamma^\mu\gamma^5(\partial^\nu\boldsymbol{\chi}^C) = \boldsymbol{\chi}^T\mathcal{C}\gamma^\mu\gamma^5\mathcal{C}(\partial^\nu\bar{\boldsymbol{\chi}}^T)\\
&= -(\partial^\nu\bar{\boldsymbol{\chi}})\mathcal{C}^T(\gamma^\mu\gamma^5)^T\mathcal{C}^T\boldsymbol{\chi} = (\partial^\nu\bar{\boldsymbol{\chi}})\mathcal{C}^{-1}(\gamma^\mu\gamma^5)^T\mathcal{C}\boldsymbol{\chi} = (\partial^\nu\bar{\boldsymbol{\chi}})\gamma^\mu\gamma^5\boldsymbol{\chi}\,,
\end{aligned} \tag{A.18}$$

where in the last line the first minus sign, coming from the transposition of spinors, gets absorbed by $\mathcal{C}^T = \mathcal{C}^{-1} = -\mathcal{C}$; in the final step we made use of $\mathcal{C}^{-1}(\gamma^\mu\gamma^5)^T\mathcal{C} = \gamma^\mu\gamma^5$. A similar relation can be derived for $\bar{\chi}\gamma^\mu(\partial^\nu\chi)$. The difference in sign comes from $\mathcal{C}^{-1}(\gamma^\mu)^T\mathcal{C} = -\gamma^\mu$.

JHEP11(2016)069

$\boxed{{}_8\mathcal{F}_\psi^{V\,\prime}}$ Here we have

$$C'_\psi \chi^\dagger \bar\sigma^\mu \chi \left[(\partial^\nu \psi^\dagger)\bar\sigma_\mu (\partial^\nu \psi)\right] \equiv \left(\xi_1^\dagger \bar\sigma^\mu \xi_1 \;\; \eta_1^\dagger \bar\sigma^\mu \eta_1\right) \underbrace{\begin{pmatrix} C'^{11}_\psi & C'^{12}_\psi \\ C'^{21}_\psi & C'^{22}_\psi \end{pmatrix}}_{C'_\psi \in \mathbb{R}} \begin{pmatrix} (\partial^\nu \xi_2^\dagger)\bar\sigma_\mu (\partial_\nu \xi_2) \\ (\partial^\nu \eta_2^\dagger)\bar\sigma_\mu (\partial_\nu \eta_2) \end{pmatrix} ,$$

$$\begin{aligned} &= C'_{VV} \bar{\boldsymbol{\chi}} \gamma^\mu \boldsymbol{\chi} \left[(\partial^\nu \bar\Psi)\gamma_\mu (\partial_\nu \Psi)\right] + C'_{VA} \bar{\boldsymbol{\chi}} \gamma^\mu \boldsymbol{\chi} \left[(\partial^\nu \bar\Psi)\gamma_\mu \gamma^5 (\partial_\nu \Psi)\right] \\ &\quad + C'_{AV} \bar{\boldsymbol{\chi}} \gamma^\mu \gamma^5 \boldsymbol{\chi} \left[(\partial^\nu \bar\Psi)\gamma_\mu (\partial_\nu \Psi)\right] + C'_{AA} \bar{\boldsymbol{\chi}} \gamma^\mu \gamma^5 \boldsymbol{\chi} \left[(\partial^\nu \bar\Psi)\gamma_\mu \gamma^5 (\partial_\nu \Psi)\right] , \end{aligned} \tag{A.24}$$

where the coefficients defined as in eqs. (A.6)–(A.7) with $c \to C'$. This simplifies in the case of Goldstino DM, where only the two CP-preserving combinations C'_{AV} and C'_{AA} survive.[23] In the following, we refer to the two associated effective operators with the notation $[{}_8\mathcal{F}_\psi^{V\,\prime}]_{AV,AA}$.

$\boxed{{}_8\mathcal{F}_V^{\not g}}$ Interactions without derivatives in the DM current involve the following operator in matrix form

$$\begin{aligned} C_V^{\not g} \chi\chi V^a_{\mu\nu} V^{a\,\mu\nu} &\equiv \left(C^{\not g}_{V,1} \eta_1 \xi_1 + C^{\not g}_{V,1} \xi_1^\dagger \eta_1^\dagger\right) V^a_{\mu\nu} V^{a\,\mu\nu} \\ &= \left[\frac{1}{2}\left(C^{\not g}_{V,1} + C^{\not g}_{V,2}\right) \bar{\boldsymbol{\chi}}\boldsymbol{\chi} + \frac{1}{2}\left(-C^{\not g}_{V,1} + C^{\not g}_{V,2}\right) \bar{\boldsymbol{\chi}}\gamma^5 \boldsymbol{\chi}\right] V^a_{\mu\nu} V^{a\,\mu\nu} . \end{aligned} \tag{A.27}$$

Clearly, only the first term is CP-preserving. CP-invariance, therefore, is preserved by imposing in eq. (A.27) the condition $C^{\not g}_{V,1} = C^{\not g}_{V,2}$. We refer to this operator with the notation $[{}_8\mathcal{F}_V^{\not g}]_V$. Here, the only subscript refers to chirality in the DM current. In the following, we focus on the interactions with gluons, $V = G$.

$\boxed{{}_8\mathcal{F}_V}$ This is a novel structure to this analysis and we shall discuss it more extensively.

$$C_V \chi^\dagger \bar\sigma^\mu (\partial^\nu \chi) V^a_{\mu\rho} V^{a\,\rho}_\nu \equiv \left[C_{V,1} \xi_1^\dagger \bar\sigma^\mu (\partial^\nu \xi_1) + C_{V,2} \eta_1^\dagger \bar\sigma^\mu (\partial^\nu \eta_1)\right] V^a_{\mu\rho} V^{a\,\rho}_\nu + h.c. \tag{A.28}$$

$$= \left[\frac{1}{2}\left(C_{V,1} - C_{V,2}\right) \bar{\boldsymbol{\chi}}\gamma^\mu (\partial^\nu \boldsymbol{\chi}) + \frac{1}{2}\left(-C_{V,1} - C_{V,2}\right) \bar{\boldsymbol{\chi}}\gamma^\mu\gamma^5 (\partial^\nu \boldsymbol{\chi})\right] V^a_{\mu\rho} V^{a\,\rho}_\nu + h.c. . \tag{A.29}$$

Considering explicitly the hermitian conjugation, we have the following structures

$$\begin{aligned} &\left[C_V \bar{\boldsymbol{\chi}}\gamma^\mu (\partial^\nu \boldsymbol{\chi}) + C_V^* (\partial^\nu \bar{\boldsymbol{\chi}})\gamma^\mu \boldsymbol{\chi}\right] V^a_{\mu\rho} V^{a\,\rho}_\nu , \qquad C_V \equiv \frac{1}{2}(C_{V,1} - C_{V,2}) \\ &\left[C_A \bar{\boldsymbol{\chi}}\gamma^\mu\gamma^5 (\partial^\nu \boldsymbol{\chi}) + C_A^* (\partial^\nu \bar{\boldsymbol{\chi}})\gamma^\mu\gamma^5 \boldsymbol{\chi}\right] V^a_{\mu\rho} V^{a\,\rho}_\nu , \quad C_A \equiv -\frac{1}{2}(C_{V,1} + C_{V,2}) \end{aligned} \tag{A.30}$$

Now, under CP, $CP\{V^a_{\mu\rho} V^{a\,\rho}_\nu\} = (-1)^\mu (-1)^\nu V^a_{\mu\rho} V^{a\,\rho}_\nu$ and $CP\{\bar{\boldsymbol{\chi}}\Gamma^\mu (\partial^\nu \boldsymbol{\chi}) \mp (\partial^\nu \bar{\boldsymbol{\chi}})\Gamma^\mu \boldsymbol{\chi}\} = (\pm)(-1)^\mu (-1)^\nu [\bar{\boldsymbol{\chi}}\Gamma^\mu (\partial^\nu \boldsymbol{\chi}) \mp (\partial^\nu \bar{\boldsymbol{\chi}})\Gamma^\mu \boldsymbol{\chi}]$, with both $\Gamma^\mu = \gamma^\mu, \gamma^\mu\gamma^5$. Imposing the restrictions

[23] The CP transformation properties follow from

$$CP\left\{\bar{\boldsymbol{\chi}}\gamma^\mu\gamma^5 \boldsymbol{\chi}\right\} = (-1)(-1)^\mu \bar{\boldsymbol{\chi}}\gamma^\mu\gamma^5 \boldsymbol{\chi} , \tag{A.25}$$

$$CP\left\{(\partial_\nu \Psi)\Gamma_\mu (\partial^\nu \Psi)\right\} = (-1)(-1)^\mu (\partial_\nu \Psi)\Gamma_\mu (\partial^\nu \Psi) , \tag{A.26}$$

with both $\Gamma^\mu = \gamma^\mu, \gamma^\mu\gamma^5$.

JHEP11(2016)069

$C_A = -C_A^* \to \mathbb{R}(C_A) = 0$ and $C_V = -C_V^* \to \mathbb{R}(C_V) = 0$ (which amount to take pure imaginary coefficients $C_{V,i=1,2}$ in eq. (A.28)), we have, in the case of Dirac DM, two possible CP-invariant combinations

$$\begin{aligned} &iC_V \left[\bar{\boldsymbol{\chi}}\gamma^\mu(\partial^\nu \boldsymbol{\chi}) - (\partial^\nu \bar{\boldsymbol{\chi}})\gamma^\mu \boldsymbol{\chi}\right] V^a_{\mu\rho} V^{a\,\rho}_\nu \,, && \text{CP-preserving, Dirac and Majorana DM} \\ &iC_A \left[\bar{\boldsymbol{\chi}}\gamma^\mu\gamma^5(\partial^\nu \boldsymbol{\chi}) - (\partial^\nu \bar{\boldsymbol{\chi}})\gamma^\mu\gamma^5 \boldsymbol{\chi}\right] V^a_{\mu\rho} V^{a\,\rho}_\nu \,, && \text{CP-preserving, Dirac DM} \end{aligned} \tag{A.31}$$

The effective operator in eq. (A.28) is present also for the case of Goldstino DM. Because of the Majorana nature of the Goldstino (see footnote 22) we are left with only one CP-invariant combination in eq. (A.31). In the following, we refer to eq. (A.31) with the notation $[{}_8\mathcal{F}_V]^{\mathcal{D}}_{V,A}$ for the two operators with Dirac DM, and $[{}_8\mathcal{F}_V]^{\mathcal{M}}_{V}$ for the only structure present in the Majorana case.

Relic density. Let us discuss in more detail why for the vector operators $[{}_8\mathcal{F}_V]^{\mathcal{D},\mathcal{M}}_V$ annihilation in p-wave is allowed, while for the operator $[{}_8\mathcal{F}_V]^{\mathcal{D}}_A$ only annihilation in d-wave is possible, as mentioned in the text. Our argument goes as follows. First, note that the traceless tensor gluon operator has $J = 2$. Conservation of total angular momentum imposes $J = 2$ also in the initial state. Since the total spin of the two annihilating DM particle is either $S = 0$ or $S = 1$, we have three possibilities. If $S = 0$, from $J = 2$ it follows that the only allowed value of total orbital angular momentum is $L = 2$ (d-wave). Note that in this case charge conjugation and parity are, respectively, $C = 1$, $P = 1$. If $S = 1$, we have two cases since the condition $J = 2$ restricts the value of total orbital angular momentum to $L = 1$ (p-wave, with $C = 1$, $P = 1$), $L = 2$ (d-wave, with $C = 1$, $P = -1$). Now, the DM current in the operator eq. (A.31), describes the annihilation of two DM particles with ingoing momenta $k_{1,2}$. In momentum space

$$[\bar{\boldsymbol{\chi}}\Gamma^\mu(\partial^\nu \boldsymbol{\chi}) - (\partial^\nu \bar{\boldsymbol{\chi}})\Gamma^\mu \boldsymbol{\chi}] \quad \Longrightarrow \quad (k_1 - k_2)^\nu \bar{\boldsymbol{\chi}}\Gamma^\mu \boldsymbol{\chi} \,, \qquad \text{with} \;\; \Gamma^\mu = \gamma^\mu, \gamma^\mu\gamma^5 \,. \tag{A.32}$$

It is possible to extract the velocity-dependence of the two factor $(k_1 - k_2)^\nu$ and $\bar{\boldsymbol{\chi}}\Gamma^\mu\boldsymbol{\chi}$ separately. The kinematic in the initial state implies $k_{1,2} = (\sqrt{s}/2, 0, 0, \pm\sqrt{s}v_{\rm rel}/4)$, with $s = 4m_\chi^2/(1 - v_{\rm rel}^2/4)$. As a consequence, only the spatial part of $(k_1 - k_2)^\nu$ is non-zero, and we have $(k_1 - k_2)^i \sim v_{\rm rel}$. As far as the DM current is concerned, in the non-relativistic limit the velocity-independent terms are $\bar{\boldsymbol{\chi}}\gamma^j\boldsymbol{\chi}$ and $\bar{\boldsymbol{\chi}}\gamma^0\gamma^5\boldsymbol{\chi}$. All in all, a p-wave contribution to the annihilation cross section can be generated only by the combinations $(k_1 - k_2)^i\bar{\boldsymbol{\chi}}\gamma^j\boldsymbol{\chi}$ and $(k_1 - k_2)^i\bar{\boldsymbol{\chi}}\gamma^0\gamma^5\boldsymbol{\chi}$. Under CP transformation we have $CP\{\bar{\boldsymbol{\chi}}\gamma^j\boldsymbol{\chi}\} = 1$, $CP\{\bar{\boldsymbol{\chi}}\gamma^0\gamma^5\boldsymbol{\chi}\} = -1$; as a consequence, the axial-vector structure cannot give a p-wave cross section (since, as discussed above, it would require $CP = 1$). We thus reproduce eqs. (3.10) and (3.11).

A.3 Scalar DM: effective operators in matrix form

$\boxed{{}_6\boldsymbol{\mathcal{S}}^{\boldsymbol{V}}_{\boldsymbol{\psi}}}$ At $D = 6$, the effective coupling with SM fermions is

$$\begin{aligned} c^V_\psi \phi^\dagger \partial_\mu \phi \psi^\dagger \bar{\sigma}^\mu \psi &\equiv \phi^\dagger(\partial_\mu \phi)\left(c^V_{\psi,1}\xi_2^\dagger \bar{\sigma}^\mu \xi_2 + c^V_{\psi,2}\eta_2^\dagger \bar{\sigma}^\mu \eta_2\right) + h.c. \\ &= \left[c_V \phi^\dagger(\partial_\mu \phi) + (c_V)^*(\partial_\mu \phi^\dagger)\phi\right]\bar{\Psi}\gamma^\mu\Psi + \left[c_A \phi^\dagger(\partial_\mu \phi) + (c_A)^*(\partial_\mu \phi^\dagger)\phi\right]\bar{\Psi}\gamma^\mu\gamma^5\Psi \,, \end{aligned} \tag{A.33}$$

JHEP11(2016)069

where we defined $c_V \equiv (c^V_{\psi,1} - c^V_{\psi,2})/2$, $c_A \equiv (-c^V_{\psi,1} - c^V_{\psi,2})/2$. We now impose CP-invariance: as already discussed, on the SM side we have $CP\left\{\bar{\Psi}\Gamma^\mu\Psi\right\} = (-1)(-1)^\mu\bar{\Psi}\Gamma^\mu\Psi$, and on the DM side, $CP\left\{\phi^\dagger(\partial^\mu\phi) - (\partial^\mu\phi^\dagger)\phi\right\} = (-1)(-1)^\mu[\phi^\dagger(\partial^\mu\phi) - (\partial^\mu\phi^\dagger)\phi]$. Imposing $c_V = -(c_V)^* \to \mathbb{R}(c_V) = 0$ and $c_A = -(c_A)^* \to \mathbb{R}(c_A) = 0$, we have two possible CP-invariant combinations

$$ic_V\left[\phi^\dagger(\partial^\mu\phi) - (\partial^\mu\phi^\dagger)\phi\right]\bar{\Psi}\gamma^\mu\Psi\,, \quad ic_A\left[\phi^\dagger(\partial^\mu\phi) - (\partial^\mu\phi^\dagger)\phi\right]\bar{\Psi}\gamma^\mu\gamma^5\Psi\,,$$

We refer to these two operators with the notation $[{}_6\mathcal{S}^V_\psi]^{\mathcal{C}}_{V,A}$ (the additional upper index $\mathcal{C}$ refers to the complex scalar nature of DM); these operators vanish if DM is a real scalar.

${}_8\boldsymbol{\mathcal{S}^T_\psi}$ There are two possible combinations

$$\partial^{[\mu}\phi^\dagger\partial^{\nu]}\phi\psi^\dagger\bar{\sigma}_\mu D_\nu\psi\,, \quad \partial^{\{\mu}\phi^\dagger\partial^{\nu\}}\phi\psi^\dagger\bar{\sigma}_\mu D_\nu\psi\,, \tag{A.34}$$

with $\partial^{[\mu}\phi^\dagger\partial^{\nu]}\phi \equiv \partial^\mu\phi^\dagger\partial^\nu\phi - \partial^\nu\phi^\dagger\partial^\mu\phi$, and $\partial^{\{\mu}\phi^\dagger\partial^{\nu\}}\phi \equiv \partial^\mu\phi^\dagger\partial^\nu\phi + \partial^\nu\phi^\dagger\partial^\mu\phi$. Using the EoM and some algebra of Dirac matrices it is possible to recast the antisymmetric operator in the following form [92]

$$\partial^{[\mu}\phi^\dagger\partial^{\nu]}\phi\psi^\dagger\bar{\sigma}_\mu D_\nu\psi \quad\Longrightarrow\quad (\partial_\rho\phi^\dagger)\overset{\leftrightarrow}{\partial^\mu}(\partial^\rho\phi)\psi^\dagger\bar{\sigma}_\mu\psi\,. \tag{A.35}$$

This operator shares the same symmetries as the operator $\phi^\dagger\partial_\mu\phi\psi^\dagger\bar{\sigma}^\mu\psi$ (in particular, note that both vanish considering the case of real DM — that is the case S2 in section 3). Even without restricting the analysis to the special case of real DM, it is easy to realize that the two operators $\phi^\dagger\partial_\mu\phi\psi^\dagger\bar{\sigma}^\mu\psi$ and $(\partial_\rho\phi^\dagger)\overset{\leftrightarrow}{\partial^\mu}(\partial^\rho\phi)\psi^\dagger\bar{\sigma}_\mu\psi$ contribute to a given observable in the same way. For definiteness, let us consider the scattering process $\bar{\psi}\psi \to \phi^\dagger\phi$, with outgoing momenta $p_{1,2}$ in the final state. At $D = 6$ — considering the first operator above — the amplitude is proportional to $(p_1 - p_2)_\mu\psi^\dagger\bar{\sigma}^\mu\psi$; on the contrary, at $D = 8$, the operator $(\partial_\rho\phi^\dagger)\overset{\leftrightarrow}{\partial^\mu}(\partial^\rho\phi)\psi^\dagger\bar{\sigma}_\mu\psi$ generates an amplitude proportional to $p_1\cdot p_2(p_1 - p_2)_\mu\psi^\dagger\bar{\sigma}^\mu\psi$. As anticipated, it follows that the two operators contribute to the analyzed observable in the same way — the operator at $D = 8$ being a $\mathcal{O}(E^2/M^2)$ correction if compared to the one at $D = 6$.

We now turn our attention to the symmetric operator in eq. (A.34). In component, we have

$$C^T_\psi\partial^\mu\phi^\dagger\partial^\nu\phi\psi^\dagger\bar{\sigma}_\mu D_\nu\psi \equiv \partial^{\{\mu}\phi^\dagger\partial^{\nu\}}\phi\left[C^T_{\psi,1}\xi^\dagger\bar{\sigma}_\mu(D_\nu\xi) + C^T_{\psi,2}\eta^\dagger\bar{\sigma}_\mu(D_\nu\eta)\right] + h.c.\,. \tag{A.36}$$

In more familiar four-component notation, we have

$$\begin{aligned}
&\partial^{\{\mu}\phi^\dagger\partial^{\nu\}}\phi\left[C_V\bar{\Psi}\gamma_\mu(\partial_\nu\Psi) + C^*_V(\partial_\nu\bar{\Psi})\gamma_\mu\Psi\right]\,, && C_V \equiv \frac{1}{2}(C^T_{\psi,1} - C^T_{\psi,2})\\
&\partial^{\{\mu}\phi^\dagger\partial^{\nu\}}\phi\left[C_A\bar{\Psi}\gamma_\mu\gamma^5(\partial_\nu\Psi) + C^*_A(\partial_\nu\bar{\Psi})\gamma_\mu\gamma^5\Psi\right]\,, && C_A \equiv -\frac{1}{2}(C^T_{\psi,1} + C^T_{\psi,2})
\end{aligned} \tag{A.37}$$

and two possible CP-invariant combinations

$$\begin{aligned}
&iC_V\partial^{\{\mu}\phi^\dagger\partial^{\nu\}}\phi\left[\bar{\Psi}\gamma_\mu(\partial_\nu\Psi) - (\partial_\nu\bar{\Psi})\gamma_\mu\Psi\right]\,, && \text{CP-preserving, complex scalar DM}\\
&iC_A\partial^{\{\mu}\phi^\dagger\partial^{\nu\}}\phi\left[\bar{\Psi}\gamma_\mu\gamma^5(\partial_\nu\Psi) - (\partial_\nu\bar{\Psi})\gamma_\mu\gamma^5\Psi\right]\,, && \text{CP-preserving, complex scalar DM}
\end{aligned} \tag{A.38}$$

JHEP11(2016)069

with real coefficients C. In the case of real scalar DM, $\partial^{\{\mu}\phi^\dagger\partial^{\nu\}}\phi = 2(\partial^\mu\phi)(\partial^\nu\phi)$. We refer to the two operators in eq. (A.38) with the notation $[{}_8\mathcal{S}^T_\psi]_{V,A}$. As a rule of thumb, the cross section for real scalar DM is four time larger if compared with the complex case.

Relic density. The annihilation cross section has a d-wave suppression since the tensor structure in the SM current implies $J = 2$ while the two annihilating scalar particles have $S = 0$, thus forcing $L = 2$ in the initial state in order to conserve the total angular momentum. By direct computation, we find eq. (3.16).

B The event generation and analysis workflow

As opposed to previous studies, where pure monojet events were studied [23], we recast a recent analysis by ATLAS [69] which allows for multiple jets. The cuts require at least one jet with a $p_T > 120\,\text{GeV}$ and allow for any number of additional jets. In particular it allows for jets with a lower p_T i.e. soft and/or collinear jets. It is well known that a generation at Matrix Element (ME) level cannot accurately generate events with soft or collinear jets. A two step generation is therefore inevitable. This section gives a detailed account of the data generation workflow. We will also discuss the implementation of the analysis and we will discuss some subtleties that are specific to a consistent EFT analysis.

We used FeynRules 2.0 [96] to create the model files. For Dirac fermions and scalars this is very straight forward. There are however difficulties with four fermion vertices including Majorana fermions. This problem has two possible solutions, both giving the same result. We can introduced a new very heavy mediator with zero decay width. Choosing the mass of this new particle very high we assure that introducing this new particle in the model does not alter the interaction and that our effective field theory picture still applies. Note that in this case we have to absorb the mass of the mediator in the vertex in order to be left with exactly the same structure as for the EFT. Or, we can run the simulation with Dirac fermions instead and keep track of the factor 4 that arise as a difference in the cross section between Dirac and Majorana fermions. For the present work we chose the latter option.

The model files are passed to MADGRAPH5 [97] interfaced with PYTHIA-6 [98]. MADGRAPH5 generates events at ME level which are then passed to PYTHIA-6 for parton showering and hadronisation. As multiple jets are allowed by the selection cuts chosen in [69] we have to generate events with an arbitrary number of jets. In [69] it was pointed out that it is sufficient to only generate 0-, 1- and 2-jet events at ME level and let PYTHIA generate the remaining arbitrary number of jets. The matching and merging procedure which is necessary under this circumstances will veto a substantial part of the created events. In order to still get enough statistics and because the signal regions used in [69] include very high missing E_T we have perform a binned data generation. For the present study we chose three bins in H_T: $H_T^1 < 250\,\text{GeV} < H_T^2 < 600\,\text{GeV} < H_T^3$. We simulate 50k events in each bin, resulting in 150k events per DM mass. The scan over the mass of the DM is performed in an interval from 1 GeV to 1 TeV.

For the analysis we need to have access to the events at parton and reconstructed level. We need the event at parton level because we have to determine the relevant energy

JHEP11(2016)069

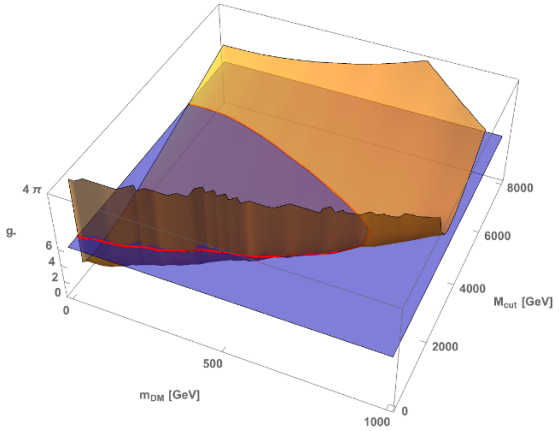

Figure 7. The yellow surface shows the constraints on g_*. Values larger (above) the yellow surface are excluded. We can infer the constraints on the physical scale of the dark mediator by intersecting the yellow surface with the blue surface representing a fixed value of g_*.

of the event, which, as discussed in the text, we chose to be $\sqrt{\hat{s}}$. The information at the reconstructed level is used for the recast of the ATLAS search [69], where the selection cuts and the signal regions are defined in terms of the observables at the reconstructed level. MadAnalyis5 [99] provides the framework needed for this analysis. In MadAnalysis expert mode we can have access to both levels of information at the same time. An example of the main and analyzer C++ files can be found on GitHub.

For each value of the DM mass we scan over $M_{\rm cut}$ ranging from 10 GeV to 8 TeV. This results in a consistent limit on g_* for each value of m_{DM} and $M_{\rm cut}$ which can then easily be inverted. By assuming that the physical scale of new physics M is also the scale $M_{\rm cut}$ up to which we can trust the EFT expansion (i.e. we saturate the EFT validity requirement), we obtain a consistent limit on M for each value of the DM mass and the coupling g_*. Figure 7 gives a graphical account of the procedure. The figure also shows very nicely the need for strongly coupled theories in the context of collider DM searches.

References

[1] Q.-H. Cao, C.-R. Chen, C.S. Li and H. Zhang, *Effective dark matter model: relic density, CDMS II, Fermi LAT and LHC*, *JHEP* **08** (2011) 018 [arXiv:0912.4511] [INSPIRE].

[2] M. Beltrán, D. Hooper, E.W. Kolb, Z.A.C. Krusberg and T.M.P. Tait, *Maverick dark matter at colliders*, *JHEP* **09** (2010) 037 [arXiv:1002.4137] [INSPIRE].

[3] Y. Bai, P.J. Fox and R. Harnik, *The Tevatron at the frontier of dark matter direct detection*, *JHEP* **12** (2010) 048 [arXiv:1005.3797] [INSPIRE].

[4] P.J. Fox, R. Harnik, J. Kopp and Y. Tsai, *Missing energy signatures of dark matter at the LHC*, *Phys. Rev.* **D 85** (2012) 056011 [arXiv:1109.4398] [INSPIRE].

JHEP11(2016)069

[5] J. Goodman, M. Ibe, A. Rajaraman, W. Shepherd, T.M.P. Tait and H.-B. Yu, *Constraints on light Majorana dark matter from colliders*, *Phys. Lett.* **B 695** (2011) 185 [arXiv:1005.1286] [INSPIRE].

[6] N. Arkani-Hamed et al., *MARMOSET: the path from LHC data to the new Standard Model via on-shell effective theories*, hep-ph/0703088 [INSPIRE].

[7] J. Alwall, P. Schuster and N. Toro, *Simplified models for a first characterization of new physics at the LHC*, *Phys. Rev.* **D 79** (2009) 075020 [arXiv:0810.3921] [INSPIRE].

[8] A. De Simone, G.F. Giudice and A. Strumia, *Benchmarks for dark matter searches at the LHC*, *JHEP* **06** (2014) 081 [arXiv:1402.6287] [INSPIRE].

[9] G. Busoni et al., *Recommendations on presenting LHC searches for missing transverse energy signals using simplified s-channel models of dark matter*, arXiv:1603.04156 [INSPIRE].

[10] A. De Simone and T. Jacques, *Simplified models vs. effective field theory approaches in dark matter searches*, *Eur. Phys. J.* **C 76** (2016) 367 [arXiv:1603.08002] [INSPIRE].

[11] F. Kahlhoefer, K. Schmidt-Hoberg, T. Schwetz and S. Vogl, *Implications of unitarity and gauge invariance for simplified dark matter models*, *JHEP* **02** (2016) 016 [arXiv:1510.02110] [INSPIRE].

[12] C. Englert, M. McCullough and M. Spannowsky, *S-channel dark matter simplified models and unitarity*, *Phys. Dark Univ.* **14** (2016) 48 [arXiv:1604.07975] [INSPIRE].

[13] J. Abdallah et al., *Simplified models for dark matter and missing energy searches at the LHC*, arXiv:1409.2893 [INSPIRE].

[14] A. Manohar and H. Georgi, *Chiral quarks and the nonrelativistic quark model*, *Nucl. Phys.* **B 234** (1984) 189 [INSPIRE].

[15] H. Georgi and L. Randall, *Flavor conserving CP-violation in invisible axion models*, *Nucl. Phys.* **B 276** (1986) 241 [INSPIRE].

[16] A.G. Cohen, D.B. Kaplan and A.E. Nelson, *Counting 4π's in strongly coupled supersymmetry*, *Phys. Lett.* **B 412** (1997) 301 [hep-ph/9706275] [INSPIRE].

[17] M.A. Luty, *Naive dimensional analysis and supersymmetry*, *Phys. Rev.* **D 57** (1998) 1531 [hep-ph/9706235] [INSPIRE].

[18] G.F. Giudice, C. Grojean, A. Pomarol and R. Rattazzi, *The strongly-interacting light Higgs*, *JHEP* **06** (2007) 045 [hep-ph/0703164] [INSPIRE].

[19] D. Liu, A. Pomarol, R. Rattazzi and F. Riva, *Patterns of strong coupling for LHC searches*, arXiv:1603.03064 [INSPIRE].

[20] R. Contino, A. Falkowski, F. Goertz, C. Grojean and F. Riva, *On the validity of the effective field theory approach to SM precision tests*, *JHEP* **07** (2016) 144 [arXiv:1604.06444] [INSPIRE].

[21] G.D. Kribs and E.T. Neil, *Review of strongly-coupled composite dark matter models and lattice simulations*, *Int. J. Mod. Phys.* **A 31** (2016) 1643004 [arXiv:1604.04627] [INSPIRE].

[22] S. Bruggisser, F. Riva and A. Urbano, *Strongly interacting light dark matter*, arXiv:1607.02474 [INSPIRE].

[23] D. Racco, A. Wulzer and F. Zwirner, *Robust collider limits on heavy-mediator dark matter*, *JHEP* **05** (2015) 009 [arXiv:1502.04701] [INSPIRE].

JHEP11(2016)069

[24] F. D'Eramo, B.J. Kavanagh and P. Panci, *You can hide but you have to run: direct detection with vector mediators*, *JHEP* **08** (2016) 111 [arXiv:1605.04917] [INSPIRE].

[25] S.R. Coleman, J. Wess and B. Zumino, *Structure of phenomenological Lagrangians.* 1, *Phys. Rev.* **177** (1969) 2239 [INSPIRE].

[26] C.G. Callan Jr., S.R. Coleman, J. Wess and B. Zumino, *Structure of phenomenological Lagrangians.* 2, *Phys. Rev.* **177** (1969) 2247 [INSPIRE].

[27] R. Casalbuoni, S. De Curtis, D. Dominici, F. Feruglio and R. Gatto, *Nonlinear realization of supersymmetry algebra from supersymmetric constraint*, *Phys. Lett.* **B 220** (1989) 569 [INSPIRE].

[28] T.E. Clark and S.T. Love, *Goldstino couplings to matter*, *Phys. Rev.* **D 54** (1996) 5723 [hep-ph/9608243] [INSPIRE].

[29] A. Brignole, F. Feruglio and F. Zwirner, *Aspects of spontaneously broken $N = 1$ global supersymmetry in the presence of gauge interactions*, *Nucl. Phys.* **B 501** (1997) 332 [hep-ph/9703286] [INSPIRE].

[30] Z. Komargodski and N. Seiberg, *From linear SUSY to constrained superfields*, *JHEP* **09** (2009) 066 [arXiv:0907.2441] [INSPIRE].

[31] C. Cheung, Y. Nomura and J. Thaler, *Goldstini*, *JHEP* **03** (2010) 073 [arXiv:1002.1967] [INSPIRE].

[32] C. Cheung, J. Mardon, Y. Nomura and J. Thaler, *A definitive signal of multiple supersymmetry breaking*, *JHEP* **07** (2010) 035 [arXiv:1004.4637] [INSPIRE].

[33] T.E. Clark, T. Lee, S.T. Love and G.-H. Wu, *On the interactions of light gravitinos*, *Phys. Rev.* **D 57** (1998) 5912 [hep-ph/9712353] [INSPIRE].

[34] A. Monin and F. Riva, *N non-linear supersymmetries*, in preparation.

[35] S. Weinberg, *Goldstone bosons as fractional cosmic neutrinos*, *Phys. Rev. Lett.* **110** (2013) 241301 [arXiv:1305.1971] [INSPIRE].

[36] C. Kilic, T. Okui and R. Sundrum, *Vectorlike confinement at the LHC*, *JHEP* **02** (2010) 018 [arXiv:0906.0577] [INSPIRE].

[37] O. Antipin, M. Redi and A. Strumia, *Dynamical generation of the weak and dark matter scales from strong interactions*, *JHEP* **01** (2015) 157 [arXiv:1410.1817] [INSPIRE].

[38] A. Belyaev, M.T. Frandsen, S. Sarkar and F. Sannino, *Mixed dark matter from technicolor*, *Phys. Rev.* **D 83** (2011) 015007 [arXiv:1007.4839] [INSPIRE].

[39] A. Hietanen, R. Lewis, C. Pica and F. Sannino, *Composite Goldstone dark matter: experimental predictions from the lattice*, *JHEP* **12** (2014) 130 [arXiv:1308.4130] [INSPIRE].

[40] A. Carmona and M. Chala, *Composite dark sectors*, *JHEP* **06** (2015) 105 [arXiv:1504.00332] [INSPIRE].

[41] S. Bhattacharya, B. Melić and J. Wudka, *Pionic dark matter*, *JHEP* **02** (2014) 115 [arXiv:1307.2647] [INSPIRE].

[42] B. Gripaios, A. Pomarol, F. Riva and J. Serra, *Beyond the minimal composite Higgs model*, *JHEP* **04** (2009) 070 [arXiv:0902.1483] [INSPIRE].

[43] M. Frigerio, A. Pomarol, F. Riva and A. Urbano, *Composite scalar dark matter*, *JHEP* **07** (2012) 015 [arXiv:1204.2808] [INSPIRE].

JHEP11(2016)069

[44] D. Marzocca and A. Urbano, *Composite dark matter and LHC interplay*, *JHEP* **07** (2014) 107 [arXiv:1404.7419] [INSPIRE].

[45] M. Chala, $h \to \gamma\gamma$ *excess and dark matter from composite Higgs models*, *JHEP* **01** (2013) 122 [arXiv:1210.6208] [INSPIRE].

[46] M. Chala, G. Nardini and I. Sobolev, *Unified explanation for dark matter and electroweak baryogenesis with direct detection and gravitational wave signatures*, *Phys. Rev.* **D 94** (2016) 055006 [arXiv:1605.08663] [INSPIRE].

[47] D.B. Kaplan, *Flavor at SSC energies: a new mechanism for dynamically generated fermion masses*, *Nucl. Phys.* **B 365** (1991) 259 [INSPIRE].

[48] R. Contino, Y. Nomura and A. Pomarol, *Higgs as a holographic pseudo-Goldstone boson*, *Nucl. Phys.* **B 671** (2003) 148 [hep-ph/0306259] [INSPIRE].

[49] K. Agashe, R. Contino and A. Pomarol, *The minimal composite Higgs model*, *Nucl. Phys.* **B 719** (2005) 165 [hep-ph/0412089] [INSPIRE].

[50] J. Mrazek, A. Pomarol, R. Rattazzi, M. Redi, J. Serra and A. Wulzer, *The other natural two Higgs doublet model*, *Nucl. Phys.* **B 853** (2011) 1 [arXiv:1105.5403] [INSPIRE].

[51] A. Pomarol and F. Riva, *The composite Higgs and light resonance connection*, *JHEP* **08** (2012) 135 [arXiv:1205.6434] [INSPIRE].

[52] A. Pomarol and J. Serra, *Top quark compositeness: feasibility and implications*, *Phys. Rev.* **D 78** (2008) 074026 [arXiv:0806.3247] [INSPIRE].

[53] U. Haisch and E. Re, *Simplified dark matter top-quark interactions at the LHC*, *JHEP* **06** (2015) 078 [arXiv:1503.00691] [INSPIRE].

[54] M. Duch, B. Grzadkowski and J. Wudka, *Classification of effective operators for interactions between the Standard Model and dark matter*, *JHEP* **05** (2015) 116 [arXiv:1412.0520] [INSPIRE].

[55] R. Foadi, M.T. Frandsen and F. Sannino, *Technicolor dark matter*, *Phys. Rev.* **D 80** (2009) 037702 [arXiv:0812.3406] [INSPIRE].

[56] M. Chala, F. Kahlhoefer, M. McCullough, G. Nardini and K. Schmidt-Hoberg, *Constraining dark sectors with monojets and dijets*, *JHEP* **07** (2015) 089 [arXiv:1503.05916] [INSPIRE].

[57] R.C. Cotta, J.L. Hewett, M.P. Le and T.G. Rizzo, *Bounds on dark matter interactions with electroweak gauge bosons*, *Phys. Rev.* **D 88** (2013) 116009 [arXiv:1210.0525] [INSPIRE].

[58] J. Brooke, M.R. Buckley, P. Dunne, B. Penning, J. Tamanas and M. Zgubic, *Vector boson fusion searches for dark matter at the LHC*, *Phys. Rev.* **D 93** (2016) 113013 [arXiv:1603.07739] [INSPIRE].

[59] S. Davidson, *Including the Z in an effective field theory for dark matter at the LHC*, *JHEP* **10** (2014) 084 [arXiv:1403.5161] [INSPIRE].

[60] A. Crivellin, U. Haisch and A. Hibbs, *LHC constraints on gauge boson couplings to dark matter*, *Phys. Rev.* **D 91** (2015) 074028 [arXiv:1501.00907] [INSPIRE].

[61] A. Biekötter, A. Knochel, M. Krämer, D. Liu and F. Riva, *Vices and virtues of Higgs effective field theories at large energy*, *Phys. Rev.* **D 91** (2015) 055029 [arXiv:1406.7320] [INSPIRE].

[62] G. Busoni, A. De Simone, E. Morgante and A. Riotto, *On the validity of the effective field theory for dark matter searches at the LHC*, *Phys. Lett.* **B 728** (2014) 412 [arXiv:1307.2253] [INSPIRE].

JHEP11(2016)069

[63] G. Busoni, A. De Simone, J. Gramling, E. Morgante and A. Riotto, *On the validity of the effective field theory for dark matter searches at the LHC, part II: complete analysis for the s-channel*, *JCAP* **06** (2014) 060 [arXiv:1402.1275] [INSPIRE].

[64] G. Busoni, A. De Simone, T. Jacques, E. Morgante and A. Riotto, *On the validity of the effective field theory for dark matter searches at the LHC part III: analysis for the t-channel*, *JCAP* **09** (2014) 022 [arXiv:1405.3101] [INSPIRE].

[65] M. Papucci, A. Vichi and K.M. Zurek, *Monojet versus the rest of the world I: t-channel models*, *JHEP* **11** (2014) 024 [arXiv:1402.2285] [INSPIRE].

[66] ATLAS collaboration, *Search for new phenomena with the monojet and missing transverse momentum signature using the ATLAS detector in* $\sqrt{s} = 7$ *TeV proton-proton collisions*, *Phys. Lett.* **B 705** (2011) 294 [arXiv:1106.5327] [INSPIRE].

[67] ATLAS collaboration, *Search for dark matter candidates and large extra dimensions in events with a jet and missing transverse momentum with the ATLAS detector*, *JHEP* **04** (2013) 075 [arXiv:1210.4491] [INSPIRE].

[68] ATLAS collaboration, *Search for new phenomena in monojet plus missing transverse momentum final states using* $10\,\text{fb}^{-1}$ *of pp collisions at* $\sqrt{s} = 8$ *TeV with the ATLAS detector at the LHC*, ATLAS-CONF-2012-147, CERN, Geneva Switzerland (2012).

[69] ATLAS collaboration, *Search for new phenomena in final states with an energetic jet and large missing transverse momentum in pp collisions at* $\sqrt{s} = 8$ *TeV with the ATLAS detector*, *Eur. Phys. J.* **C 75** (2015) 299 [*Erratum ibid.* **C 75** (2015) 408] [arXiv:1502.01518] [INSPIRE].

[70] CMS collaboration, *Search for new physics with a mono-jet and missing transverse energy in pp collisions at* $\sqrt{s} = 7$ *TeV*, *Phys. Rev. Lett.* **107** (2011) 201804 [arXiv:1106.4775] [INSPIRE].

[71] CMS collaboration, *Search for dark matter and large extra dimensions in monojet events in pp collisions at* $\sqrt{s} = 7$ *TeV*, *JHEP* **09** (2012) 094 [arXiv:1206.5663] [INSPIRE].

[72] CMS collaboration, *Search for dark matter, extra dimensions and unparticles in monojet events in proton-proton collisions at* $\sqrt{s} = 8$ *TeV*, *Eur. Phys. J.* **C 75** (2015) 235 [arXiv:1408.3583] [INSPIRE].

[73] PLANCK collaboration, P.A.R. Ade et al., *Planck* 2013 *results. XVI. Cosmological parameters*, *Astron. Astrophys.* **571** (2014) A16 [arXiv:1303.5076] [INSPIRE].

[74] J. Kumar and D. Marfatia, *Matrix element analyses of dark matter scattering and annihilation*, *Phys. Rev.* **D 88** (2013) 014035 [arXiv:1305.1611] [INSPIRE].

[75] XENON100 collaboration, E. Aprile et al., *Limits on spin-dependent WIMP-nucleon cross sections from* 225 *live days of XENON*100 *data*, *Phys. Rev. Lett.* **111** (2013) 021301 [arXiv:1301.6620] [INSPIRE].

[76] LUX collaboration, D.S. Akerib et al., *First results from the LUX dark matter experiment at the Sanford Underground Research Facility*, *Phys. Rev. Lett.* **112** (2014) 091303 [arXiv:1310.8214] [INSPIRE].

[77] LUX collaboration, D.S. Akerib et al., *Results on the spin-dependent scattering of weakly interacting massive particles on nucleons from the run* 3 *data of the LUX experiment*, *Phys. Rev. Lett.* **116** (2016) 161302 [arXiv:1602.03489] [INSPIRE].

JHEP11(2016)069

[78] SuperCDMS collaboration, R. Agnese et al., *New results from the search for low-mass weakly interacting massive particles with the CDMS low ionization threshold experiment*, *Phys. Rev. Lett.* **116** (2016) 071301 [arXiv:1509.02448] [INSPIRE].

[79] CRESST collaboration, G. Angloher et al., *Results on light dark matter particles with a low-threshold CRESST-II detector*, *Eur. Phys. J.* **C 76** (2016) 25 [arXiv:1509.01515] [INSPIRE].

[80] J. Fan, M. Reece and L.-T. Wang, *Non-relativistic effective theory of dark matter direct detection*, *JCAP* **11** (2010) 042 [arXiv:1008.1591] [INSPIRE].

[81] A.L. Fitzpatrick, W. Haxton, E. Katz, N. Lubbers and Y. Xu, *The effective field theory of dark matter direct detection*, *JCAP* **02** (2013) 004 [arXiv:1203.3542] [INSPIRE].

[82] M. Cirelli, E. Del Nobile and P. Panci, *Tools for model-independent bounds in direct dark matter searches*, *JCAP* **10** (2013) 019 [arXiv:1307.5955] [INSPIRE].

[83] M. Drees and M. Nojiri, *Neutralino-nucleon scattering revisited*, *Phys. Rev.* **D 48** (1993) 3483 [hep-ph/9307208] [INSPIRE].

[84] J. Hisano, K. Ishiwata and N. Nagata, *QCD effects on direct detection of wino dark matter*, *JHEP* **06** (2015) 097 [arXiv:1504.00915] [INSPIRE].

[85] J.M. Cornwall, D.N. Levin and G. Tiktopoulos, *Derivation of gauge invariance from high-energy unitarity bounds on the S matrix*, *Phys. Rev.* **D 10** (1974) 1145 [*Erratum ibid.* **D 11** (1975) 972] [INSPIRE].

[86] N. Bell, G. Busoni, A. Kobakhidze, D.M. Long and M.A. Schmidt, *Unitarisation of EFT amplitudes for dark matter searches at the LHC*, *JHEP* **08** (2016) 125 [arXiv:1606.02722] [INSPIRE].

[87] Y. Hochberg, E. Kuflik, T. Volansky and J.G. Wacker, *Mechanism for thermal relic dark matter of strongly interacting massive particles*, *Phys. Rev. Lett.* **113** (2014) 171301 [arXiv:1402.5143] [INSPIRE].

[88] N.F. Bell, Y. Cai and R.K. Leane, *Mono-W dark matter signals at the LHC: simplified model analysis*, *JCAP* **01** (2016) 051 [arXiv:1512.00476] [INSPIRE].

[89] N.F. Bell, J.B. Dent, A.J. Galea, T.D. Jacques, L.M. Krauss and T.J. Weiler, *Searching for dark matter at the LHC with a mono-Z*, *Phys. Rev.* **D 86** (2012) 096011 [arXiv:1209.0231] [INSPIRE].

[90] L. Carpenter, A. DiFranzo, M. Mulhearn, C. Shimmin, S. Tulin and D. Whiteson, *Mono-Higgs-boson: a new collider probe of dark matter*, *Phys. Rev.* **D 89** (2014) 075017 [arXiv:1312.2592] [INSPIRE].

[91] P.J. Fox, R. Harnik, J. Kopp and Y. Tsai, *LEP shines light on dark matter*, *Phys. Rev.* **D 84** (2011) 014028 [arXiv:1103.0240] [INSPIRE].

[92] B. Grzadkowski, M. Iskrzynski, M. Misiak and J. Rosiek, *Dimension-six terms in the Standard Model Lagrangian*, *JHEP* **10** (2010) 085 [arXiv:1008.4884] [INSPIRE].

[93] PICO collaboration, C. Amole et al., *Dark matter search results from the PICO-2L C_3F_8 bubble chamber*, *Phys. Rev. Lett.* **114** (2015) 231302 [arXiv:1503.00008] [INSPIRE].

[94] Super-Kamiokande collaboration, K. Choi et al., *Search for neutrinos from annihilation of captured low-mass dark matter particles in the sun by Super-Kamiokande*, *Phys. Rev. Lett.* **114** (2015) 141301 [arXiv:1503.04858] [INSPIRE].

JHEP11(2016)069

[95] IceCube collaboration, M.G. Aartsen et al., *Improved limits on dark matter annihilation in the sun with the 79-string IceCube detector and implications for supersymmetry*, *JCAP* **04** (2016) 022 [arXiv:1601.00653] [INSPIRE].

[96] A. Alloul, N.D. Christensen, C. Degrande, C. Duhr and B. Fuks, *FeynRules 2.0 — a complete toolbox for tree-level phenomenology*, *Comput. Phys. Commun.* **185** (2014) 2250 [arXiv:1310.1921] [INSPIRE].

[97] J. Alwall et al., *The automated computation of tree-level and next-to-leading order differential cross sections and their matching to parton shower simulations*, *JHEP* **07** (2014) 079 [arXiv:1405.0301] [INSPIRE].

[98] T. Sjöstrand, S. Mrenna and P.Z. Skands, *PYTHIA 6.4 physics and manual*, *JHEP* **05** (2006) 026 [hep-ph/0603175] [INSPIRE].

[99] E. Conte, B. Fuks and G. Serret, *MadAnalysis 5, a user-friendly framework for collider phenomenology*, *Comput. Phys. Commun.* **184** (2013) 222 [arXiv:1206.1599] [INSPIRE].

JHEP11(2016)069